High-Order Numerical Algorithms for Steady and Unsteady Simulation of Viscous Compressible Flow with Shocks
(Grant FA9550-07-0195)

Sachin Premasuthan, Kui Ou,
Patrice Castonguay, Lala Li, Yves Allaneau, David Williams,
Peter Vincent, and Antony Jameson

Department of Aeronautics and Astronautics
Stanford University

July 2010

This research is also supported by NSF under Grant 0915006

Support

STANFORD UNIVERSITY

- **AFOSR**
  - *Sachin Premasuthan, and Kui Ou*
- **Stanford Graduate Fellowship**
  - *Patrice Castonguay, Yves Allaneau,*
  - *Lala Li, David Williams*
- **NSF**
  - *Peter Vincent*
- **One summer month each from AFOSR and NSF**
  - *Antony Jameson*

"Buy one, Get five free."

Overview

STANFORD UNIVERSITY

1) Theoretical developments of flux reconstruction method

- *Unstructured* high-order methods
- The *Flux Reconstruction* approach
- Energy *Stable* Flux Reconstruction schemes
- *Flux Reconstruction as Filtered DG*
- Extending the formulation to *2D* and 3D

2) Applications to practical problems

- Parallelization using GPUs
- Adaptive h-p mesh refinements
- *Unsteady flow on deformable meshes*
- Implicit Large Eddy Simulation for transitional flow
- *LES Models with SD (with G.Lodato and C.H.Liang from CTR)*

Theoretical developments

STANFORD UNIVERSITY

1. Unstructured high-order methods
2. The Flux Reconstruction approach
3. Energy Stable Flux Reconstruction schemes
4. Flux Reconstruction as Filtered DG
5. Extending the formulation to 2D and 3D

Unstructured High-Order Methods

STANFORD UNIVERSITY

- *Low-order* schemes are *robust*, *mature*, *geometrically flexible* ...
- However, not well suited for applications requiring very *low numerical dissipation*
- *High-order* methods offer a solution
- *Unstructured* high-order methods can be applied in complex geometries

[1] Copyright Allen Edwards Photography www.PaloAltoPhoto.com

Unstructured High-Order Methods

STANFORD UNIVERSITY

- Essentially Non-Oscillatory (ENO), Weighted ENO (WENO), Continuous Galerkin (CG), *Discontinuous Galerkin* (DG), Spectral Volume (SV), *Spectral Difference* (SD)
- However, their use amongst a non-specialist community *remains limited* ...
- Why?
- Efficient *time integration*
- *Shock capturing*
- *Mesh generation*
- *Complexity* (at various levels)

Theoretical developments

STANFORD UNIVERSITY

1. Unstructured high-order methods
2. The Flux Reconstruction approach
3. Energy Stable Flux Reconstruction schemes
4. Flux Reconstruction as Filtered DG
5. Extending the formulation to 2D and 3D

Flux Reconstruction

STANFORD UNIVERSITY

- *Flux Reconstruction* (FR) approach first proposed by Huynh in 2007 [2]
- *Intuitive*, *simple* to implement, *unifying*
- *Nodal DG* and *SD* (at least for a linear flux) within a *single framework*
- Can produce an *infinite range* of other schemes

[2] 18th AIAA Computational Fluid Dynamics Conference, 2007 (AIAA 2007-4079)

Flux Reconstruction

STANFORD UNIVERSITY

- Consider *1D* scalar conservation law $$\frac{\partial u}{\partial t} + \frac{\partial f}{\partial x} = 0$$
- Represent solution by order *k* piecewise *discontinuous* polynomials within each element
- Represent flux by order *k+1* piecewise *continuous* polynomials within each element.

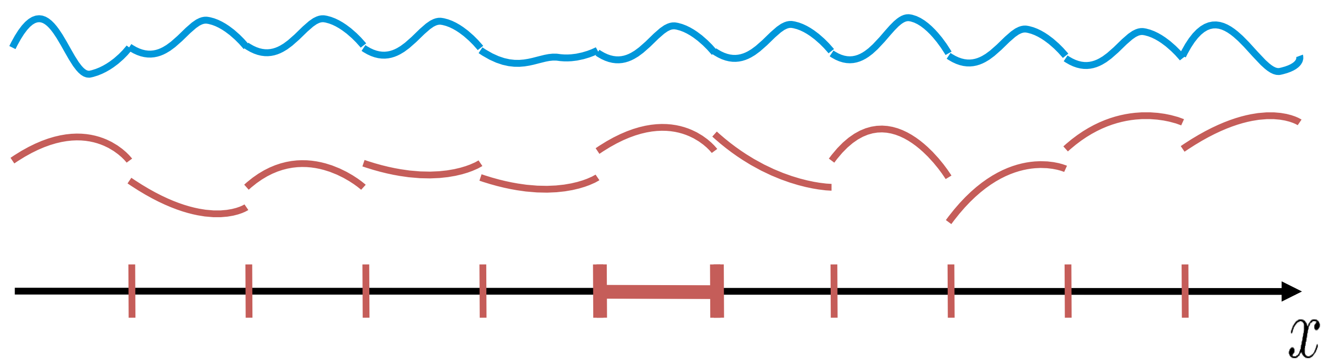

- With flux reconstruction approach, continuous flux = interior discontinuous flux function + boundary flux correction function

Procedures for Flux Reconstruction

STANFORD UNIVERSITY

- Map each element to a *'standard element'*

- Represent solution (order *k*) within standard element using a *nodal basis*

- *R*econstruct *discontinuous* flux (order *k*).
  For linear problem, this is just a scaling by a constant.

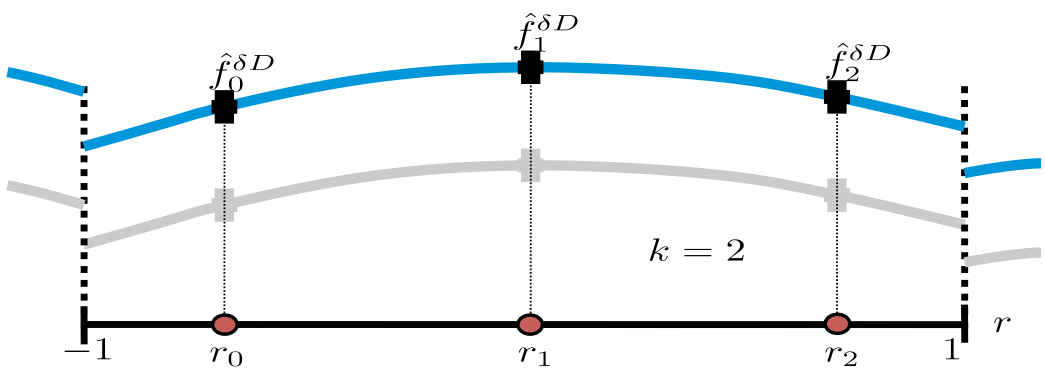

Procedures for Flux Reconstruction

- Calculate *numerical* interface fluxes and evaluate the required flux corrections
- Define an order *k+1* left *correction function scaled by the required flux correction*

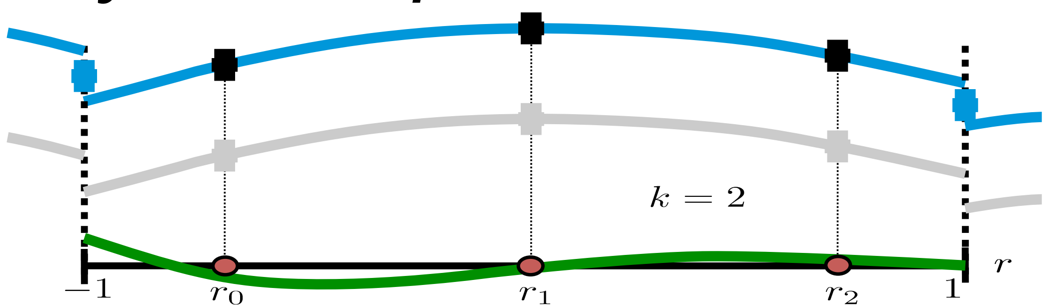

- … and *add* it to the *discontinuous flux to obtain the continuous flux*

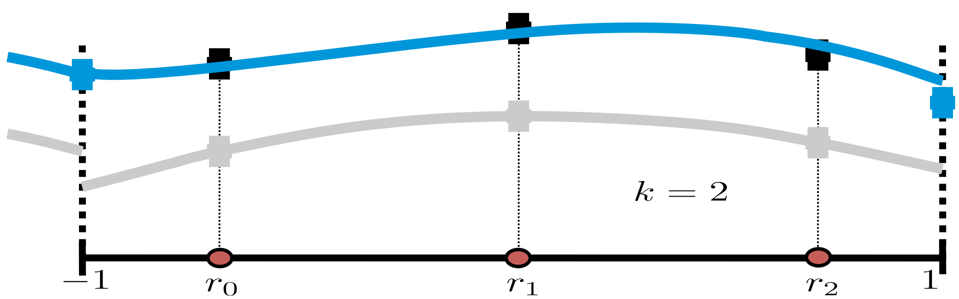

Procedures for Flux Reconstruction

STANFORD UNIVERSITY

- And do the same for the right hand side

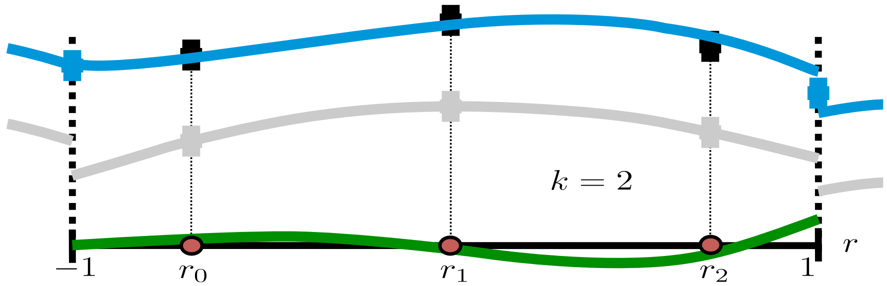

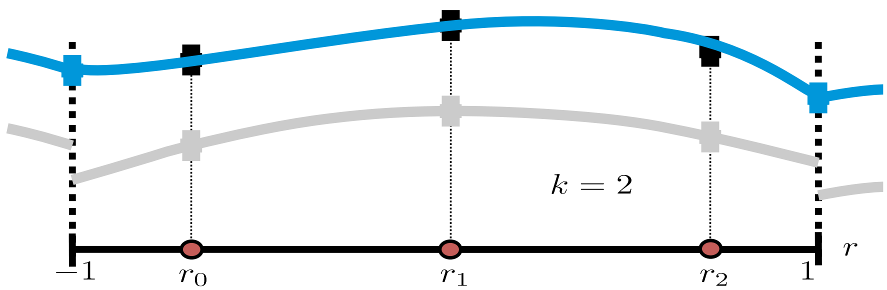

- Evaluate gradient of the *continuous* flux at solution points … and *advance* the solution in time

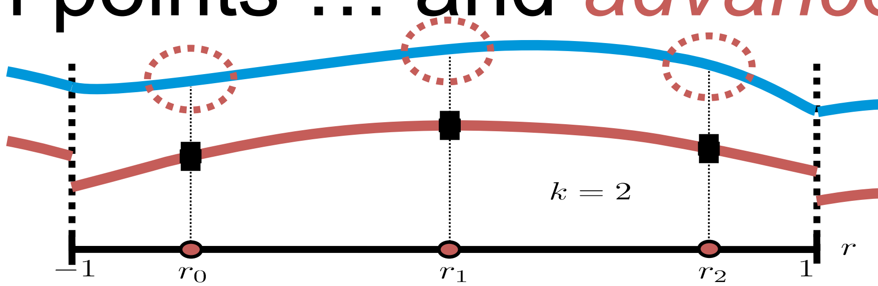

Flux Reconstruction

STANFORD UNIVERSITY

- Nature of FR scheme depends on *solution points*, *interface flux*, *correction function*
- Can recover *nodal DG, SD* (at least for a linear flux) and various *new schemes* (see Huynh [2])
- Until now, schemes have been identified on an *ad hoc* basis

[2] H. T. Huynh. 18th AIAA Computational Fluid Dynamics Conference. 2007 (AIAA 2007-4079)

Theoretical developments

STANFORD UNIVERSITY

1. Unstructured high-order methods
2. The Flux Reconstruction approach
3. Energy Stable Flux Reconstruction schemes
4. Flux Reconstruction as Filtered DG
5. Extending the formulation to 2D and 3D

Energy Stable Flux Reconstruction in 1D

STANFORD UNIVERSITY

- We have identified a range of correction functions that *guarantee energy stability* (at least for a linear flux)
- Proof based on Jameson 2010 [3]
- The 'trick' is to make an energy stability proof for FR look like the *well known proof for nodal DG*

[3] A. Jameson. Journal of Scientific Computing. 2010

Energy Stable Flux Reconstruction in 1D

STANFORD UNIVERSITY

- For *stability* we need

$$\int_{-1}^{1} r^i g_L \, \mathrm{d}r = \begin{cases} 0 & 0 \le i \le k-2 \\ \dfrac{ck!}{k}\left(\dfrac{\mathrm{d}^{k+1} g_L}{\mathrm{d}r^{k+1}}\right) & i = k-1. \end{cases}$$

$$\frac{-2}{(2k+1)(a_k k!)^2} < c < \infty \qquad a_k = \frac{(2k)!}{2^k (k!)^2}$$

- And remember, FR requires

$$g_L(-1) = 1, \qquad g_L(1) = 0$$

- *k+2* conditions for order *k+1* polynomial
- Right correction by *symmetry*
- All conditions independent of *solution basis*

Energy Stable Flux Reconstruction in 1D

STANFORD UNIVERSITY

- If satisfied then (for *1D linear advection*)

$$\frac{\mathrm{d}}{\mathrm{d}t}||u^{\delta}||_{k,2}^{2} \leq 0$$

- Where

$$||u^{\delta}||_{k,2} = \left[\sum_{n=1}^{N}\int_{x_n}^{x_{n+1}} (u_n^{\delta})^2 + \frac{c}{2}(J_n)^{2k}\left(\frac{\partial^k u_n^{\delta}}{\partial x^k}\right)^2 \mathrm{d}x\right]^{1/2}$$

- Which is a broken Sobolev type *norm* (implying *energy stability*)

Energy Stable Flux Reconstruction in 1D

STANFORD UNIVERSITY

- The aforementioned are satisfied *if*

$$g_L = \frac{(-1)^k}{2}\left[L_k - \left(\frac{\eta_k L_{k-1} + L_{k+1}}{1+\eta_k}\right)\right]$$

$$g_R = \frac{1}{2}\left[L_k + \left(\frac{\eta_k L_{k-1} + L_{k+1}}{1+\eta_k}\right)\right]$$

$$\eta_k = \frac{c(2k+1)(a_k k!)^2}{2} \qquad \frac{-2}{(2k+1)(a_k k!)^2} < c < \infty$$

- Parametrized by the single scalar *c*

What *known* schemes can we recover?

STANFORD UNIVERSITY

$$c = \frac{2(k+1)}{(2k+1)k(a_k k!)^2}$$ ▶ Huynh's 'g2' scheme

$$c = \frac{2k}{(2k+1)(k+1)(a_k k!)^2}$$ ▶ One particular SD scheme

$$c = 0$$ ▶ Nodal DG Scheme

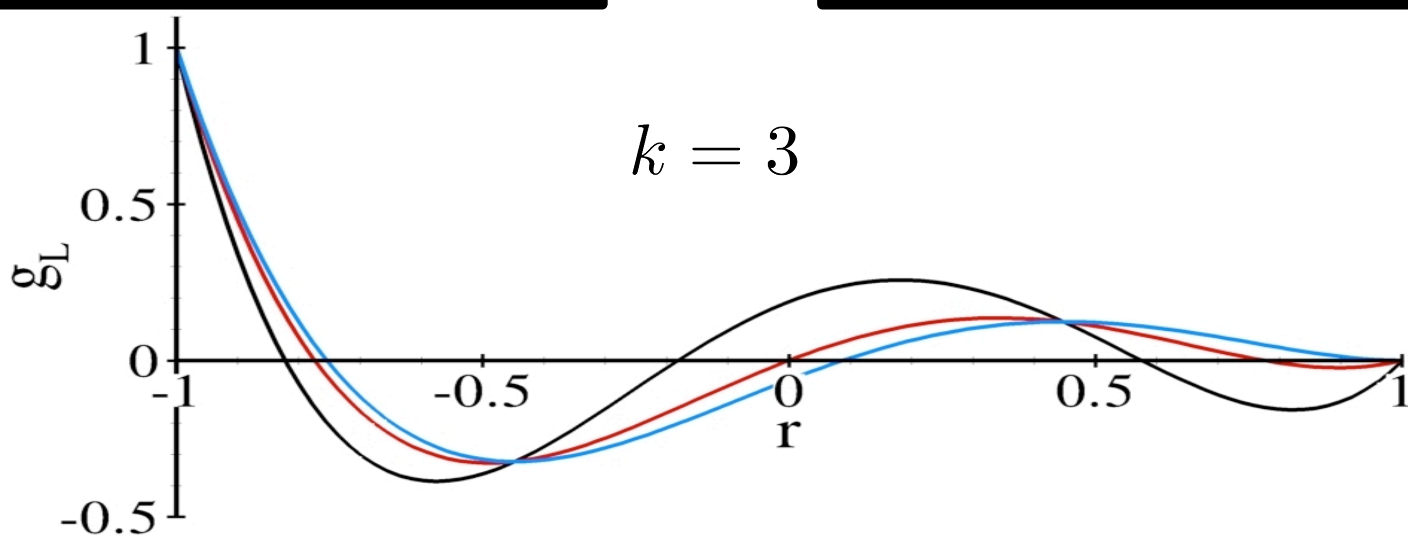

Energy Stable Flux Reconstruction in 1D

STANFORD UNIVERSITY

- Theoretical *order of accuracy* vs. 'c'
- Theoretical *CFL limit* for *RK4* scheme vs. 'c'

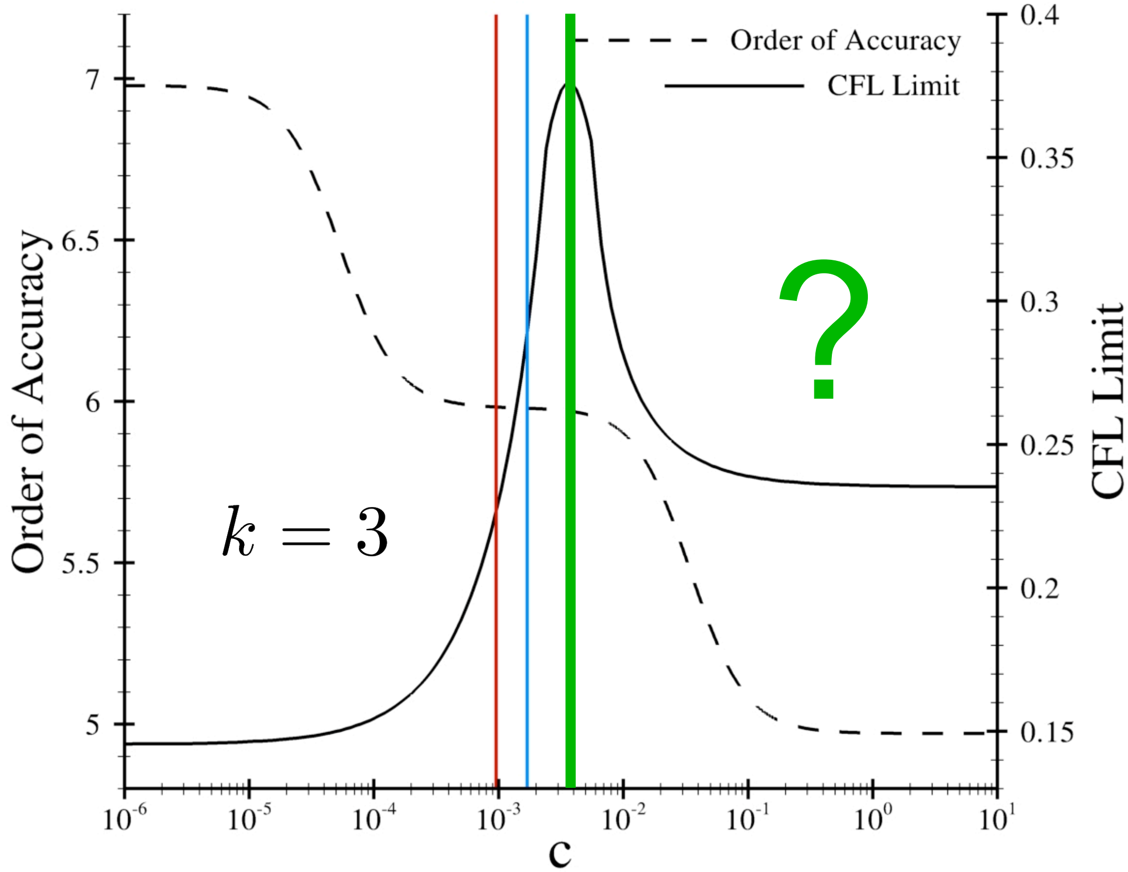

Theoretical developments

STANFORD UNIVERSITY

1. Unstructured high-order methods
2. The Flux Reconstruction approach
3. Energy Stable Flux Reconstruction schemes
4. Flux Reconstruction as Filtered DG
5. Extending the formulation to 2D and 3D

Flux Reconstruction as a filtered DG

STANFORD UNIVERSITY

Nodal DG

$$\mathbf{M}\frac{d\mathbf{u}}{dt} + a\mathbf{S}\mathbf{u} + f_{cr}\,l(1) - f_{cl}\,l(-1) = 0$$

or

$$\frac{d\mathbf{u}}{dt} = -\mathbf{M}^{-1}[a\mathbf{S}\mathbf{u} + f_{cr}\,l(1) - f_{cl}\,l(-1)]$$

The Nodal DG with Filter is

$$\frac{d\mathbf{u}}{dt} = -\mathbf{F}\mathbf{M}^{-1}[a\mathbf{S}\mathbf{u} + f_{cr}\,l(1) - f_{cl}\,l(-1)]$$

or

$$\mathbf{M}\mathbf{F}^{-1}\frac{d\mathbf{u}}{dt} + a\mathbf{S}\mathbf{u} + f_{cr}\,l(1) - f_{cl}\,l(-1) = 0$$

Flux Reconstruction as a filtered DG

STANFORD UNIVERSITY

If u and $\hat{u}$ are the nodal and modal vectors, then

$$\mathbf{u} = V\hat{\mathbf{u}}$$

$$\mathbf{F} = V\Lambda V^{-1}$$

where the entries of Λ define the damping of each mode, and V is the Vandermonde matrix. Also we have

$$\mathbf{M} = \frac{h}{2}(VV^T)^{-1} = \frac{h}{2}V^{T^{-1}}V^{-1}$$

Thus setting $MF^{-1} = \tilde{M}$,

$$\tilde{\mathbf{M}}\frac{d\mathbf{u}}{dt} + a\mathbf{S}\mathbf{u} + f_{cl}l(1) - f_{cl}l(-1) = 0$$

where

$$\tilde{\mathbf{M}} = \frac{h}{2}V^{T^{-1}}\Lambda^{-1}V^{-1} = \frac{h}{2}(V\Lambda V^T)^{-1}$$

Hence the scheme is stable in the norm

$$\sum_{cells}\frac{h}{2}u^T\tilde{M}u = \sum_{cells}\frac{h}{2}\hat{u}^T\Lambda^{-1}\hat{u}$$

Flux Reconstruction as a filtered DG

STANFORD UNIVERSITY

Flux Reconstruction expressed as a Filtered DG

$$(\mathbf{M} + cdd^T)\frac{d\mathbf{u}}{dt} + a\mathbf{S}\mathbf{u} + f_{cr}l(1) - f_{cl}l(-1) = 0$$

Factor out **M** to get

$$\mathbf{M}(I + cM^{-1}dd^T)\frac{d\mathbf{u}}{dt} + a\mathbf{S}\mathbf{u} + f_{cr}l(1) - f_{cl}l(-1) = 0$$

The filter now becomes

$$F = (I + cM^{-1}dd^T)^{-1}$$

For polynomial of degree p, we have

$$u^{(p)} = \hat{u}_p L_p^{(p)}, \; L_p = c_p x^p + \ldots, \; L_p^{(p)} = p!c_p = a_p, \; d^T = (0\ 0\ \ldots\ a_p)$$

Filter Examples

STANFORD UNIVERSITY

$$dd^T = \begin{pmatrix} 0 & & & \\ & 0 & & \\ & & \dots & \\ & & & ca_p^2 \end{pmatrix}$$

$$M^{-1} = \begin{pmatrix} R_1 & & & \\ & R_2 & & \\ & & \dots & \\ & & & R_p \end{pmatrix}$$

$$I + cM^{-1}dd^T = \begin{pmatrix} 1 & & & \\ & 1 & & \\ & & \dots & \\ & & & 1 + cR_p a_p^2 \end{pmatrix}$$

$$F = (I + cM^{-1}dd^T)^{-1} = \begin{pmatrix} 1 & & & \\ & 1 & & \\ & & \dots & \\ & & & \frac{1}{1+cR_p a_p^2} \end{pmatrix}, \text{ for SD, } = \begin{pmatrix} 1 & & & \\ & 1 & & \\ & & \dots & \\ & & & \frac{p+1}{2p+1} \end{pmatrix}$$

Theoretical developments

STANFORD UNIVERSITY

1. Unstructured high-order methods
2. The Flux Reconstruction approach
3. Energy Stable Flux Reconstruction schemes
4. Flux Reconstruction as Filtered DG
5. Extending the formulation to 2D and 3D

Energy Stable Flux Reconstruction in 2D

STANFORD UNIVERSITY

Extension of 1D to *quadrilaterals*

simple via *tensor product* basis

Extension to *triangles*

not so simple. However, triangles facilitate the meshing of *complex geometries*, so this is important

Preliminaries

STANFORD UNIVERSITY

Represent the solution using interior nodal values, with $\mathbf{x} = (x, y)$

$$u(\mathbf{x}) = \sum u_i l_i(\mathbf{x})$$

Represent the correction flux using flux mismatch at the interface and a correction function that propagates the difference into the interior.

$$g(\mathbf{x}) = \sum f_{ck} g_k(\mathbf{x})$$

Where f_{ck} is the correction flux at Each flux points at the interfaces

The governing equation can then be written in terms of the divergence of the uncorrected and correction fluxes, with $\mathbf{a} = (a, b)$ being the wave velocities vector,

$$\frac{\partial u_h}{\partial t} + \nabla \cdot (\mathbf{a} u_h) + \nabla \cdot \mathbf{g} = 0$$

Discrete Energy Estimate for Flux Reconstruction in 2D

STANFORD UNIVERSITY

$$\int_D u_h \left[\frac{\partial u_h}{\partial t} + \nabla \cdot (\mathbf{a} u_h) + \nabla \cdot \mathbf{g} \right] dA = 0$$

to get

$$\frac{d}{dt} \int_D \frac{u_h^2}{2} dA + a \int_D u_h \frac{\partial u_h}{\partial x} dA + b \int_D u_h \frac{\partial u_h}{\partial y} dA + \int_D u_h \nabla \cdot \mathbf{g} dA = 0$$

Further integration by parts to get

$$\frac{d}{dt} \int_D \frac{u_h^2}{2} dA + \int_B (\mathbf{n} \cdot \mathbf{a}) \frac{u_h^2}{2} dS + \int_B \mathbf{n} \cdot \mathbf{g} u_h dS - \int_D \mathbf{g} \cdot \nabla u_h dA = 0$$

Hence by choosing **g** suitably, we can ensure energy stability in a certain norm.

$$\underbrace{\frac{d}{dt} \int_D \frac{u_h^2}{2} dA - \int_D \mathbf{g} \cdot \nabla u_h dA}_{\text{for energy stable, this need to be non increasing}} + \int_B (\mathbf{n} \cdot \mathbf{a}) \frac{u_h^2}{2} dS + \int_B \mathbf{n} \cdot \mathbf{g} u_h dS = 0$$

Methods to Choose g to Ensure Energy Stability

STANFORD UNIVERSITY

As an example, consider a third-order method in 2D. Choose g as follows:

$$\int_D \mathbf{g} \cdot \nabla u_h dA = c_1 \; A \; u_{h\,xx} \; \frac{\partial^2}{\partial x^2} \nabla \cdot \mathbf{g} + c_2 \; A \; u_{h\,xy} \; \frac{\partial^2}{\partial xy} \nabla \cdot \mathbf{g} + c_3 \; A \; u_{h\,yy} \; \frac{\partial^2}{\partial y^2} \nabla \cdot \mathbf{g}$$

$$\frac{\partial^2}{\partial \mathbf{x}^2} \left[\frac{\partial u_h}{\partial t} + \nabla \cdot (\mathbf{a} u_h) + \nabla \cdot \mathbf{g} \right] = 0$$

The highest derivatives terms lead to this identify.

$$\frac{\partial}{\partial t} \mathbf{u}_{\mathbf{h}\,xx} + 0 + \frac{\partial^2}{\partial \mathbf{x}^2} \nabla \cdot \mathbf{g} = 0$$

Substitution yields the following, which is in the kinetic energy form, as desired

$$\int_D \mathbf{g} \cdot \nabla u_h dA = c_1 \; A \; u_{h\,xx} \; \frac{\partial}{\partial t} u_{h\,xx} + c_2 \; A \; u_{h\,xy} \; \frac{\partial}{\partial t} u_{h\,xy} + c_3 \; A \; u_{h\,yy} \; \frac{\partial}{\partial t} u_{h\,yy}$$

$$= \frac{1}{2} \frac{d}{dt} \int (c_1 \; u_{h\,xx}^2 + c_2 \; u_{h\,xy}^2 + c_3 \; u_{h\,yy}^2) dA$$

Energy Stable Flux Reconstruction in 2D

STANFORD UNIVERSITY

Hence by choosing **g** suitably, we can ensure energy stability in a certain norm.

$$\underbrace{\frac{d}{dt}\int_D \frac{u_h^2}{2} dA - \int_D \mathbf{g}\cdot\nabla u_h dA}_{\text{for energy stable, this need to be non increasing}} + \int_B (\mathbf{n}\cdot\mathbf{a})\frac{u_h^2}{2} dS + \int_B \mathbf{n}\cdot\mathbf{g} u_h dS = 0$$

$$\int_D \mathbf{g}\cdot\nabla u_h dA = c_1\ A\ u_{h_{xx}} \frac{\partial^2}{\partial x^2}\nabla\cdot\mathbf{g} + c_2\ A\ u_{h_{xy}} \frac{\partial^2}{\partial xy}\nabla\cdot\mathbf{g} + c_3\ A\ u_{h_{yy}} \frac{\partial^2}{\partial y^2}\nabla\cdot\mathbf{g}$$

Hence the energy estimate of the flux reconstruction scheme becomes

$$\underbrace{\frac{1}{2}\frac{d}{dt}\int_D \left(u_h^2 + c_1\ u_{h_{xx}}^2 + c_2\ u_{h_{xy}}^2 + c_3\ u_{h_{yy}}^2\right) dA}_{\text{energy estimate for FR}} + \int_B (\mathbf{n}\cdot\mathbf{a})\frac{u_h^2}{2} dS + \int_B \mathbf{n}\cdot\mathbf{g} u_h dS = 0$$

The Flux Reconstruction scheme is **stable in this new norm**.

Energy Stable Flux Reconstruction in 2D

STANFORD UNIVERSITY

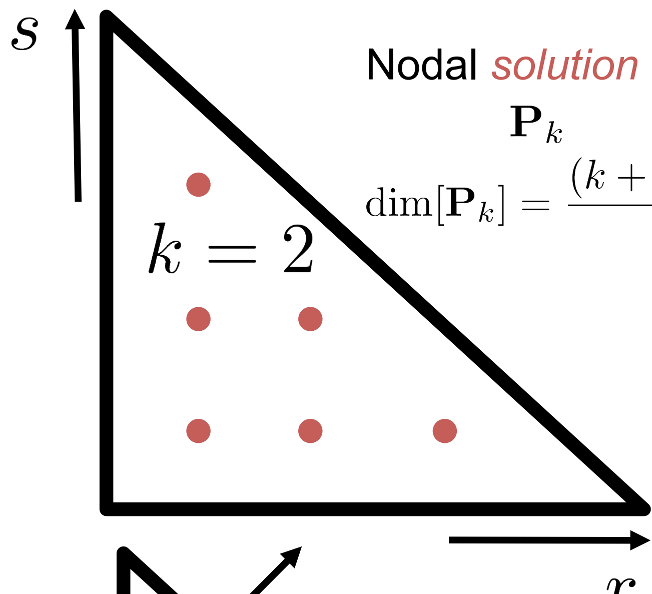

Nodal *solution* basis

$$\mathbf{P}_k$$

$$\dim[\mathbf{P}_k] = \frac{(k+1)(k+2)}{2}$$

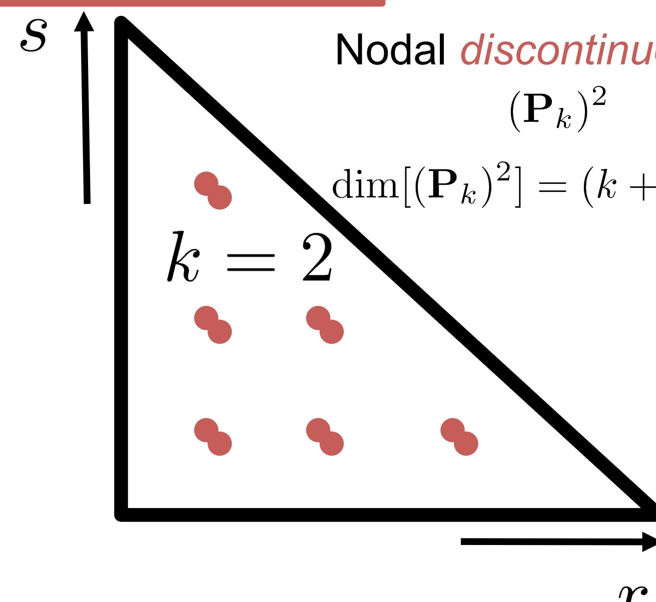

Nodal *discontinuous flux*

$$(\mathbf{P}_k)^2$$

$$\dim[(\mathbf{P}_k)^2] = (k+1)(k+2)$$

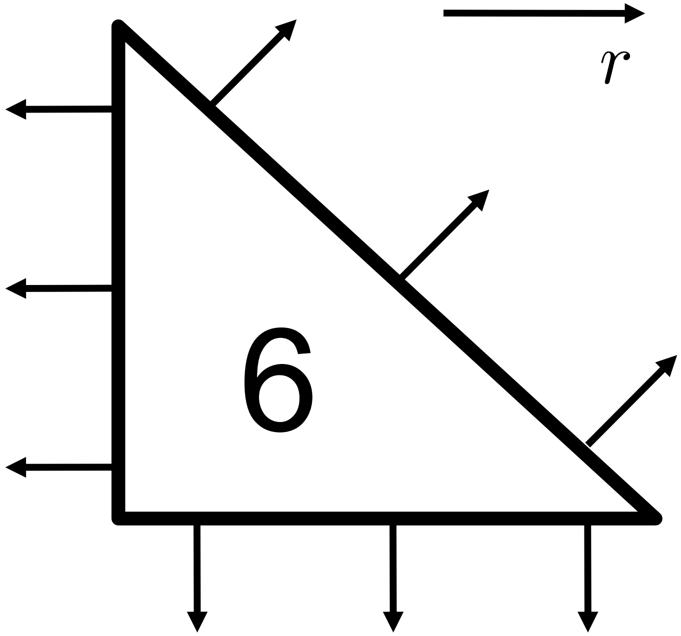

Correction functions in *Raviart-Thomas* function space

$$\mathbf{RT}_k = (\mathbf{P}_k)^2 + \begin{pmatrix} r \\ s \end{pmatrix} \overline{\mathbf{P}}_k \subset (\mathbf{P}_{k+1})^2$$

$$\dim[\mathbf{RT}_k] = (k+1)(k+3) = 3(k+1) + k(k+1)$$

Edge normal degrees of freedom fixed by flux corrections at k+1 points on each edge

Internal degrees of freedom used to set moments (to ensure energy stability)

Energy Stable Flux Reconstruction in 2D

STANFORD UNIVERSITY

then the resulting requirements are, firstly, lower moments should vanish

$$\int_D \mathbf{g} \cdot \nabla(x^p y^q) dA = 0, \text{ if p+q} < \text{k}$$

and highest moments should assume the following values

$$\int_D \mathbf{g} \cdot \nabla(x^{p_m} y^{q_m}) dA = c_m (k+2)(p_m!)^2 (q_m!)^2 \gamma_m, \text{ if } p_m\text{+}q_m = \text{k}$$

Methods to Find g or the Divergence of g

STANFORD UNIVERSITY

Applying Integration by parts, we have

$$\int_D u_h \nabla \cdot \mathbf{g} dA = \int_B \mathbf{n} \cdot \mathbf{g} u_h dS - \int_D \mathbf{g} \cdot \nabla u_h dA$$

The energy stability set the requirement for the last term, as shown previously

$$\int_D u_h \nabla \cdot \mathbf{g} dA = \int_B \mathbf{n} \cdot \mathbf{g} u_h dS - \underbrace{\int_D \mathbf{g} \cdot \nabla u_h dA}_{\text{from energy estimate}}$$

Hence we can directly solve for the divergence of the correction function $\nabla \cdot \mathbf{g}$.

$$\int_D u_h \nabla \cdot \mathbf{g} dA = \text{Boundary Integral Terms} + \text{Function of parameter } c$$

This is leads to a **one parameter family** of energy stable schemes.

Energy Stable Flux Reconstruction in 2D

STANFORD UNIVERSITY

- Energy stable correction functions are parametrized by a *single scalar*
- Resulting scheme shows similarities to *'Lifting Collocation Penalty'* method of Wang [4]
- However, (as in 1D) correction functions *guarantee energy stability*, rather than identified on an *ad hoc* basis

[4] Z. J. Wang, H. Gao. Journal of Computational Physics. 2009

Theoretical developments

1. Unstructured high-order methods
2. The Flux Reconstruction approach
3. Energy Stable Flux Reconstruction schemes
4. Flux Reconstruction as Filtered DG
5. Extending the formulation to 2D and 3D

Energy Stable Flux Reconstruction in 3D

STANFORD
UNIVERSITY

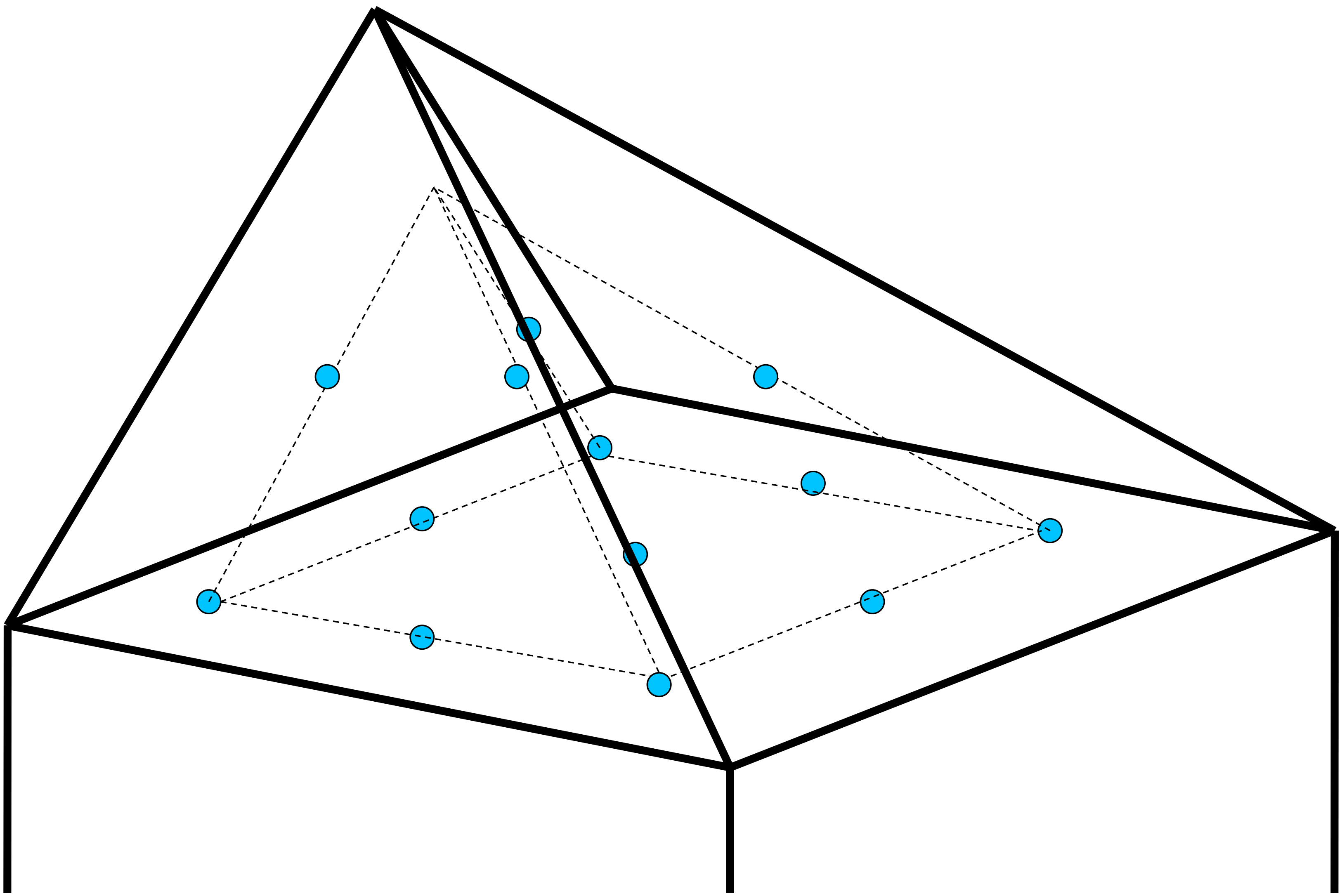

Energy Stable Flux Reconstruction for Pyramid

STANFORD UNIVERSITY

As an example, if u_h and $\nabla \cdot \mathbf{g}$ are polynomials of degree 2, then

$$\begin{aligned} u_h =& a_1 + a_2 x + a_3 y + a_4 x^2 + a_5 xy + a_6 y^2 + a_7 x^2 y + a_8 xy^2 + a_9 x^2 y^2 + \\ & a_{10} z + a_{11} xz + a_{12} yz + a_{13} z^2 + a_{14} xyz \end{aligned}$$

and

$$\begin{aligned} \nabla \cdot \mathbf{g} =& b_1 + b_2 x + b_3 y + b_4 x^2 + b_5 xy + b_6 y^2 + b_7 x^2 y + b_8 xy^2 + b_9 x^2 y^2 + \\ & b_{10} z + b_{11} xz + b_{12} yz + b_{13} z^2 + b_{14} xyz \end{aligned}$$

The energy stability for 3D pyramids requires all moments of $\mathbf{g}$ to vanish except

The Highest Moments

$$\begin{aligned} \int_D (g_x xy^2 + g_y x^2 y) dV &= 8 c_1 b_9 \\ \int_D (g_z z) dV &= 2 c_2 b_{13} \\ \int_D (g_x yz + g_y xz + g_z xy) dV &= c_3 b_{14} \end{aligned}$$

Energy Stable Flux Reconstruction for Pyramid

STANFORD UNIVERSITY

After integration by parts $\nabla \cdot \mathbf{g}$ can be determined from 14 moments

$$\int_D \nabla \cdot \mathbf{g} dV = \int \mathbf{g} \cdot \mathbf{n} dS + 0$$

$$\int_D \nabla \cdot \mathbf{g} x dV = \int \mathbf{g} \cdot \mathbf{n} x dS + 0$$

$$\int_D \nabla \cdot \mathbf{g} y dV = \int \mathbf{g} \cdot \mathbf{n} y dS + 0$$

$$\int_D \nabla \cdot \mathbf{g} z dV = \int \mathbf{g} \cdot \mathbf{n} z dS + 0$$

$$\ldots$$

$$\int_D \nabla \cdot \mathbf{g} x^2 y^2 dV = \int \mathbf{g} \cdot \mathbf{n} x^2 y^2 dS + 16 c_1 b_9$$

$$\int_D \nabla \cdot \mathbf{g} z^2 dV = \int \mathbf{g} \cdot \mathbf{n} z^2 dS + 4 c_2 b_{13}$$

$$\int_D \nabla \cdot \mathbf{g} xyz dV = \int \mathbf{g} \cdot \mathbf{n} xyz dS + c_3 b_{14}$$

14 Moments

Results

STANFORD UNIVERSITY

- Euler vortex propagating on *highly unstructured mixed mesh*
- *Third-order* solution polynomials
- *c=1/1050* (*SD scheme* for quadrilaterals)

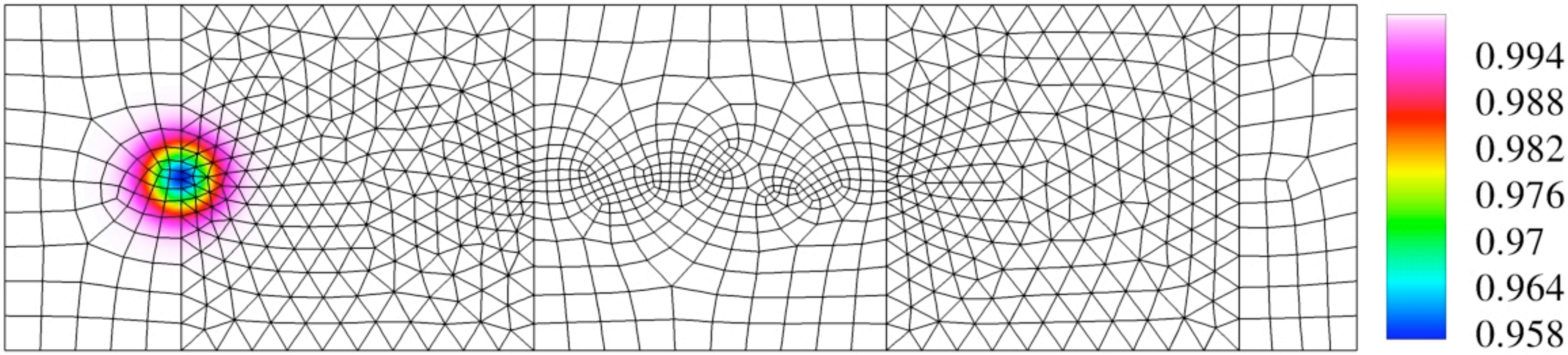

Results

STANFORD UNIVERSITY

- Euler vortex propagating on *highly unstructured mixed mesh*
- *Third-order* solution polynomials
- *c=1/1050* (*SD scheme* for quadrilaterals)

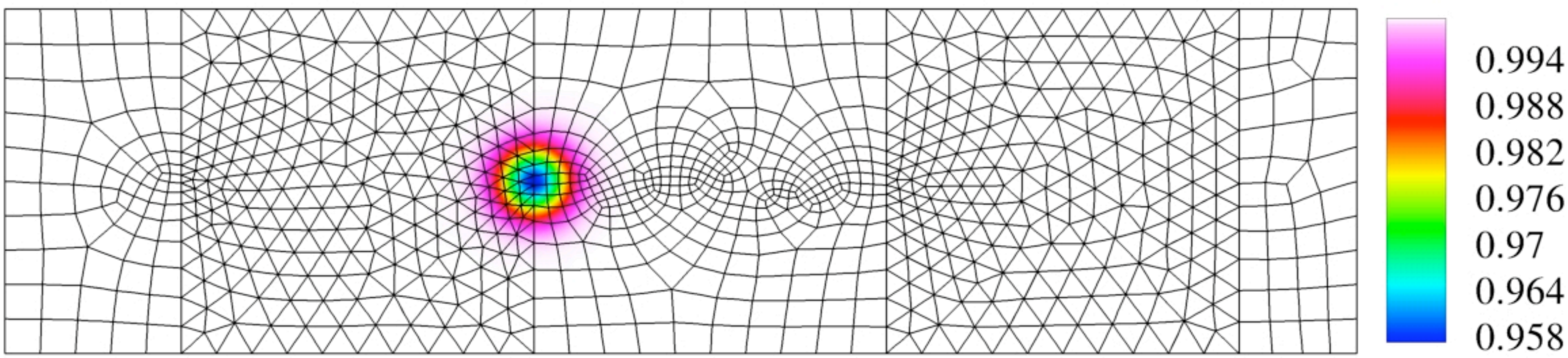

Results

STANFORD UNIVERSITY

- Euler vortex propagating on *highly unstructured mixed mesh*
- *Third-order* solution polynomials
- *c=1/1050* (*SD scheme* for quadrilaterals)

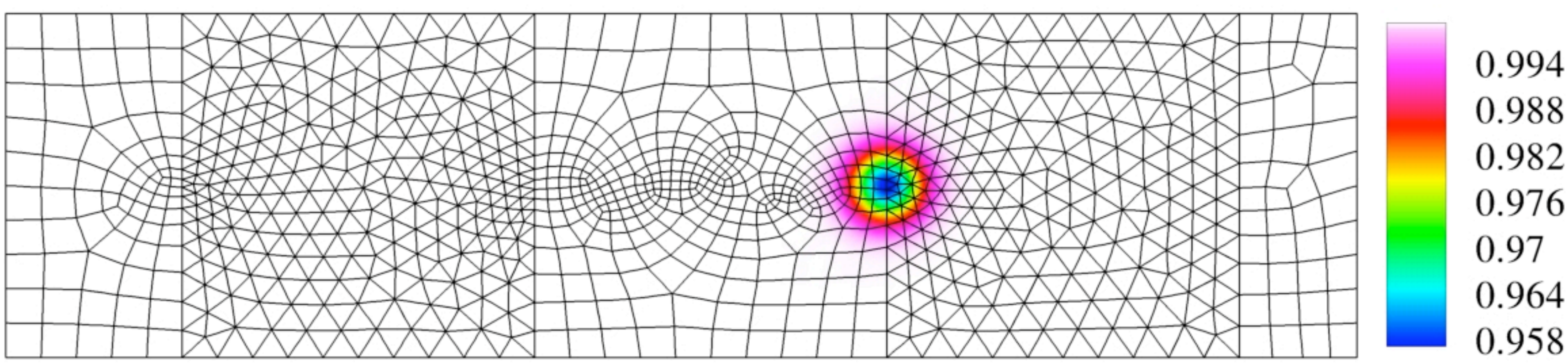

Results

STANFORD UNIVERSITY

- Euler vortex propagating on *highly unstructured mixed mesh*
- *Third-order* solution polynomials
- *c=1/1050* (*SD scheme* for quadrilaterals)

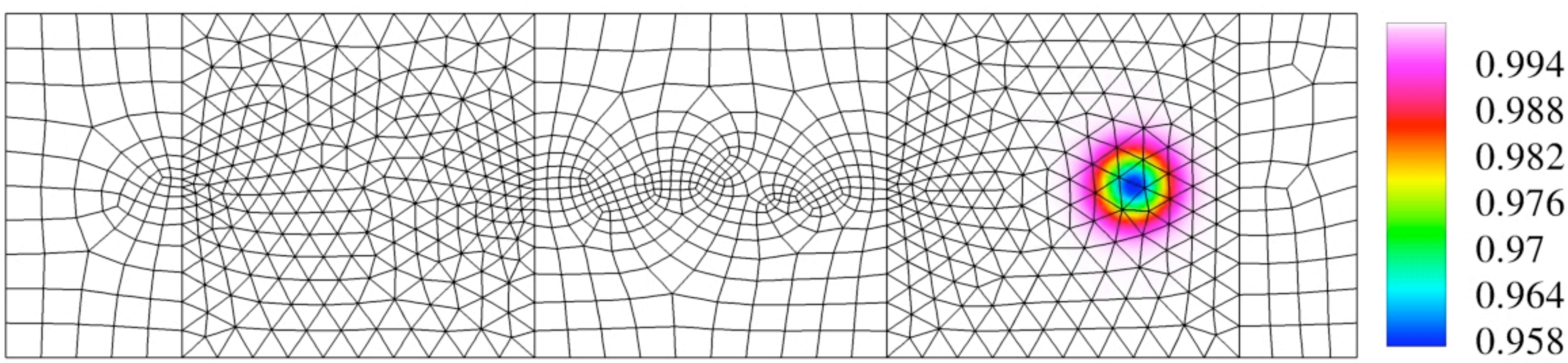

Applications

STANFORD UNIVERSITY

1. Parallelization using GPUs
2. Unsteady Flow on Deformable Meshes
3. Adaptive h-p Mesh Refinement
4. Implicit Large Eddy Simulation with SD
5. LES Models with SD

GPUs Parallelization

STANFORD UNIVERSITY

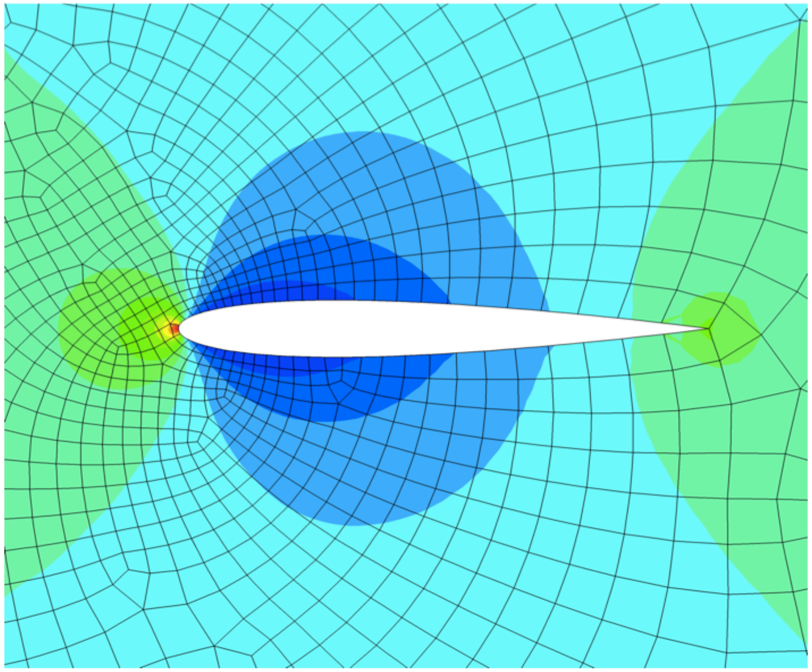

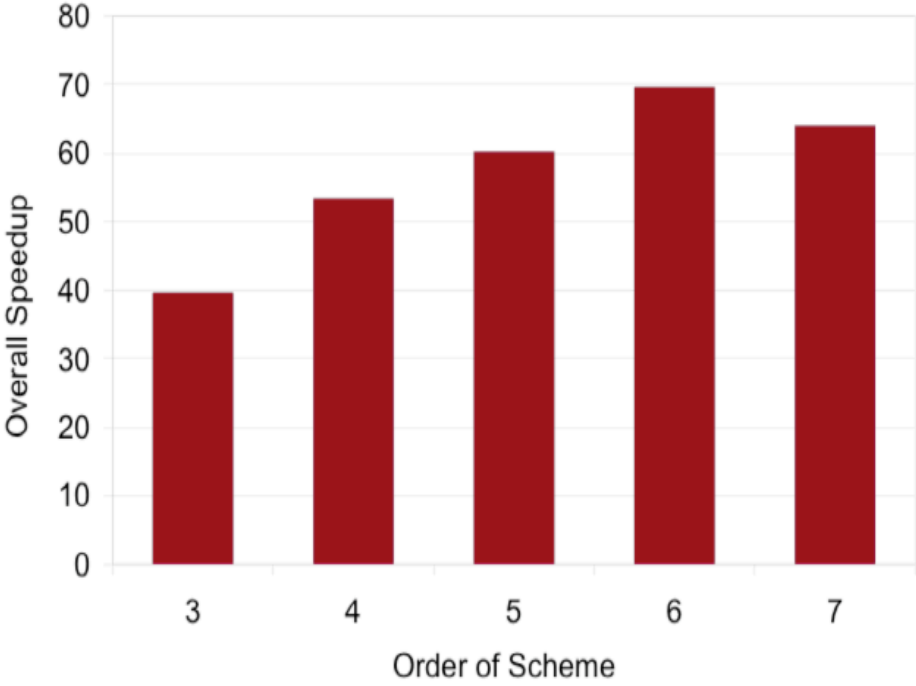

Applications

STANFORD UNIVERSITY

1. Parallelization using GPUs
2. Unsteady Flow on Deformable Meshes
3. Adaptive h-p Mesh Refinement
4. Implicit Large Eddy Simulation with SD
5. LES Models with SD

Unsteady Flow on Deformable Meshes

STANFORD UNIVERSITY

Numerical Result

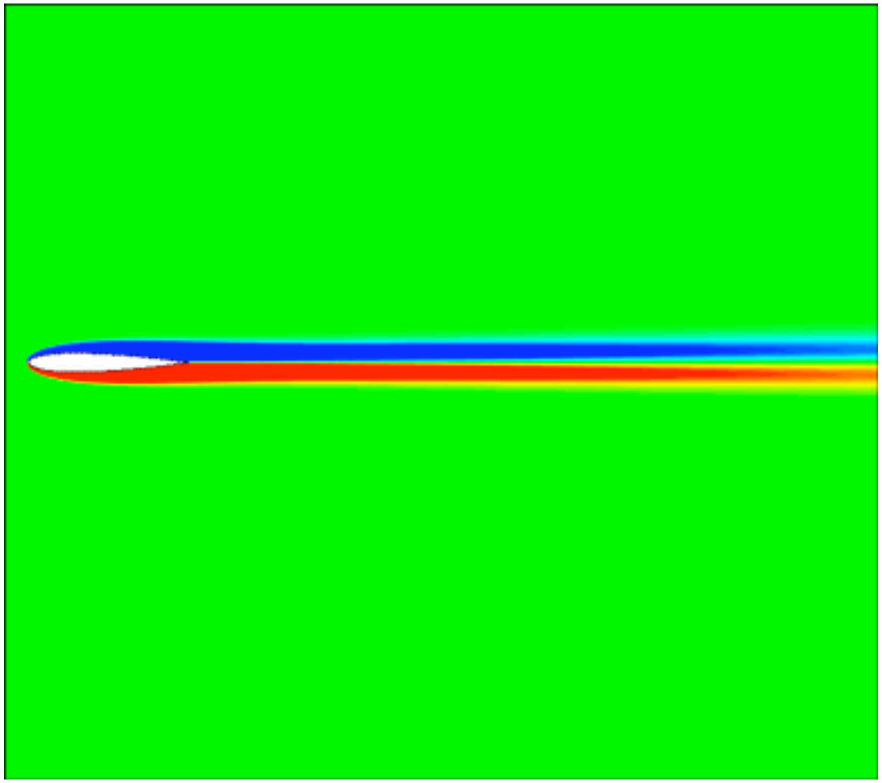

Experimental Results

Flow Conditions: M=0.2, Re=1800, Str=1.5, h=0.12c

Flow Solver: 5th order SD on deforming mesh

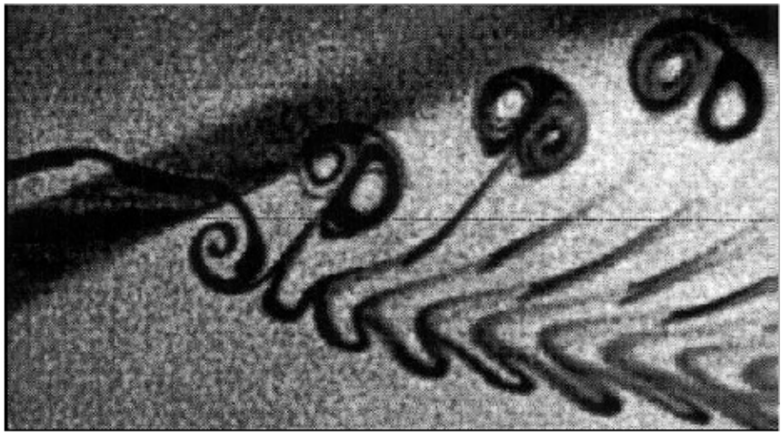

Jones, Dohring, and Platzer, “Experimental and computational investigation of the Knoller-Betz effect”, AIAA Journal, 1998

Unsteady Flow on Deformable Meshes

STANFORD UNIVERSITY

Rigid Mesh Displacement

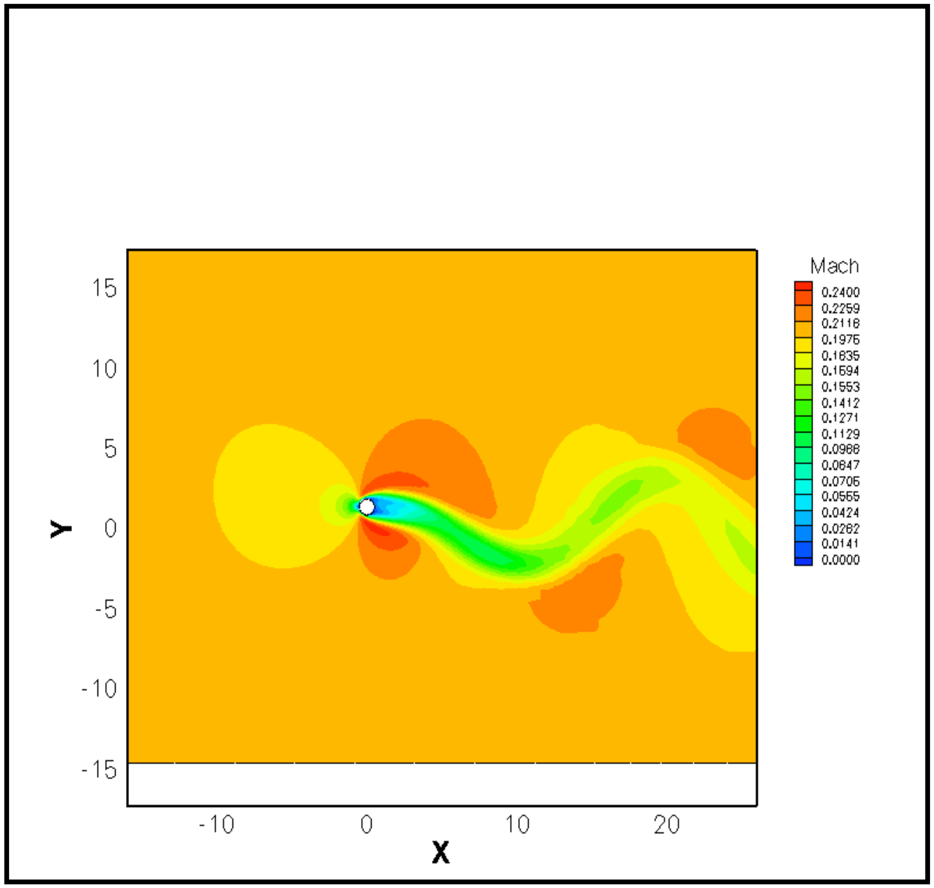

Flow Conditions: M=0.2, Re=400

Deforming Mesh

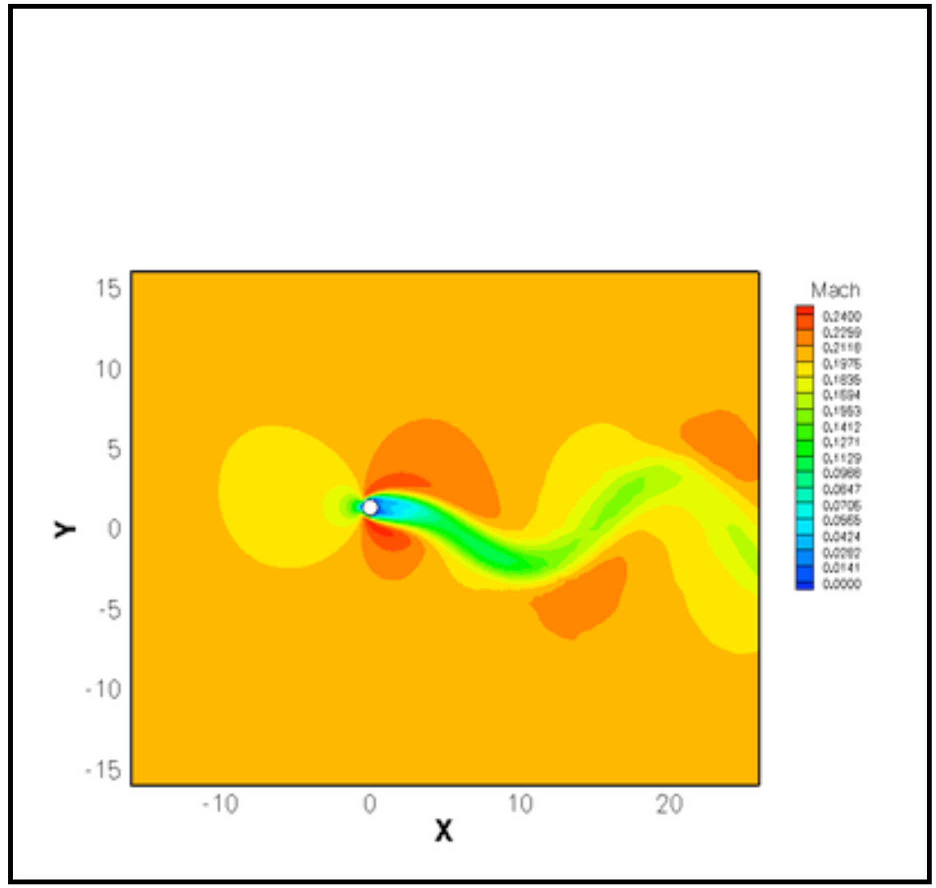

Plunging Motion: ω=0.2π, h=4/3

Unsteady Flow on Deformable Meshes

STANFORD UNIVERSITY

True Space

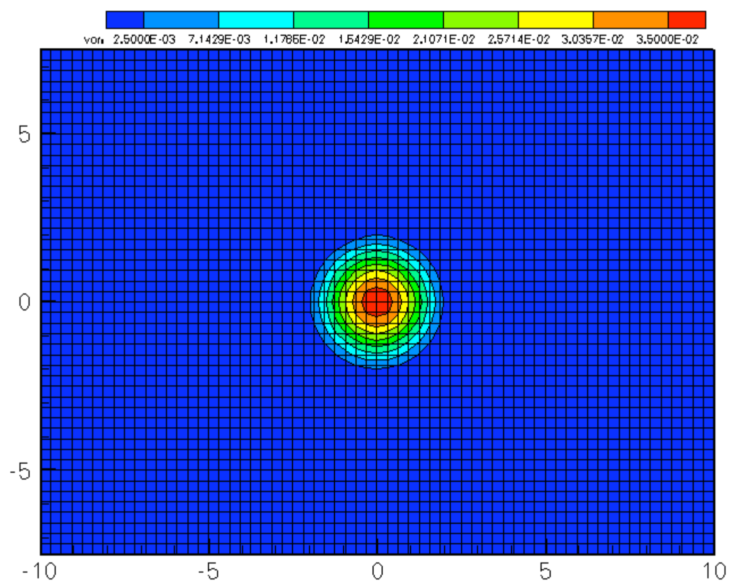

Reference Space

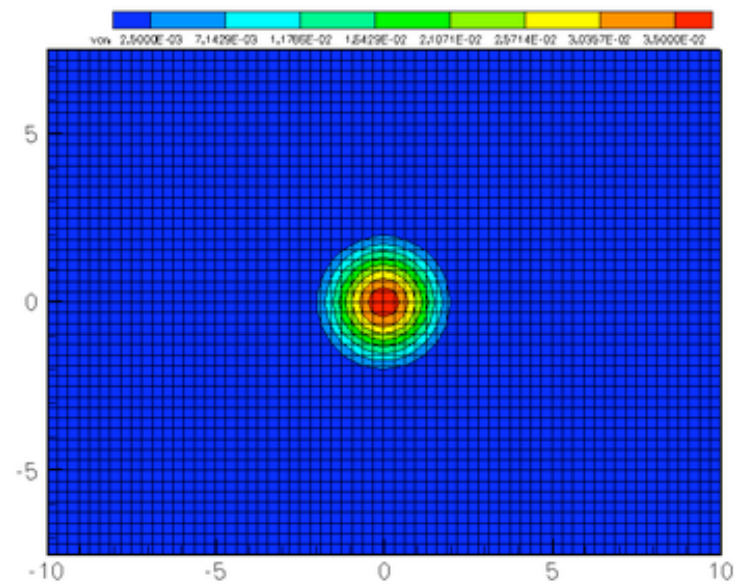

Fluid Structure Interaction Problems

STANFORD UNIVERSITY

Flow Solver Settings: Re=200, Mach=0.2, ρ=1, 4th order SD method

Structure Solver Settings: ρ=1000, E=1.4e^{6}, v=0.4

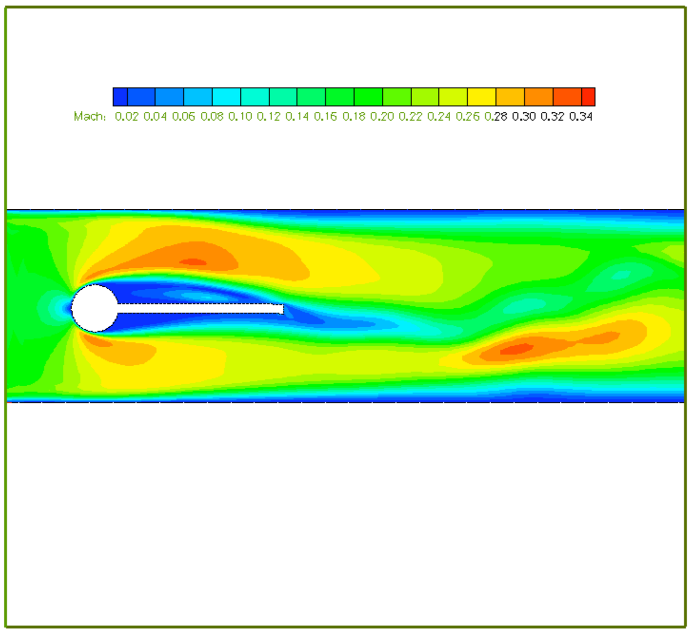

Mach Contour

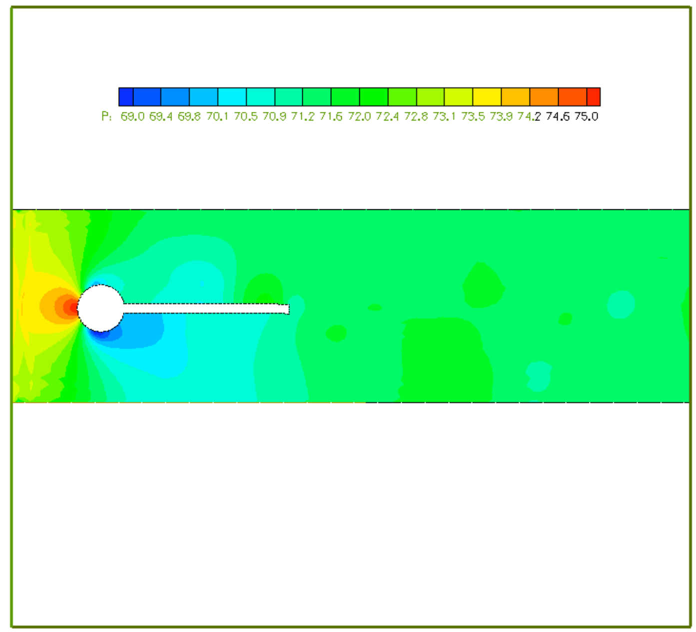

Pressure Contour

Fluid Structure Interaction Problem

STANFORD UNIVERSITY

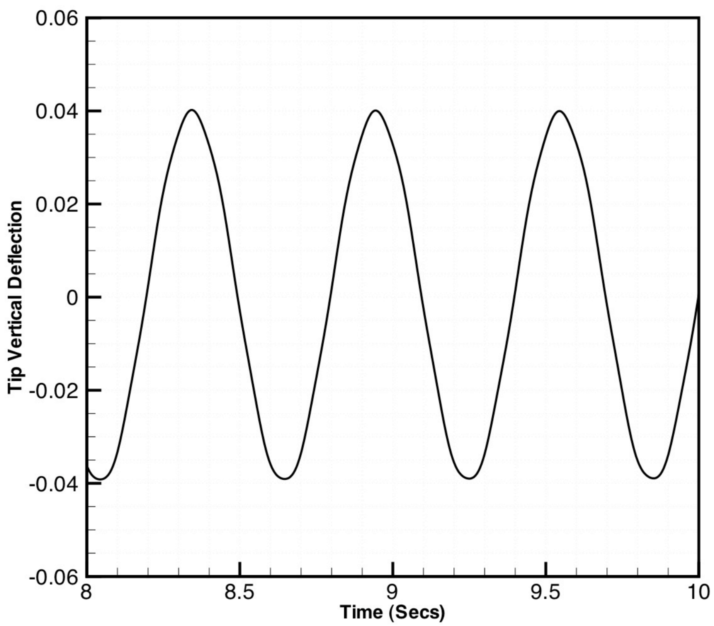

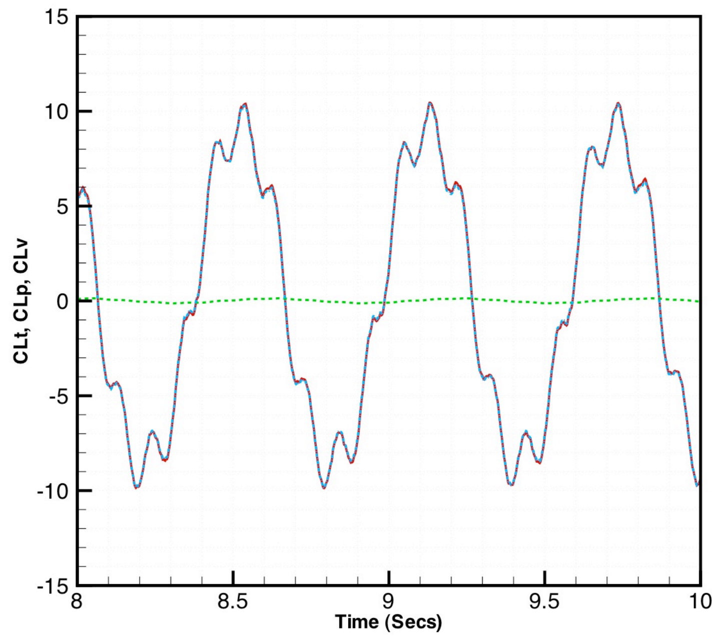

Tip Deflection (Left) and CL Time Histories (Right) for the Fluid Structure Interaction Problem. Re=200. Mach=0.2. Pressure component of CL curve is in dashed blue color. The viscous component is in green dash-dot curve. Total CL is the red solid curve.

Fluid Structure Interaction Problem

STANFORD UNIVERSITY

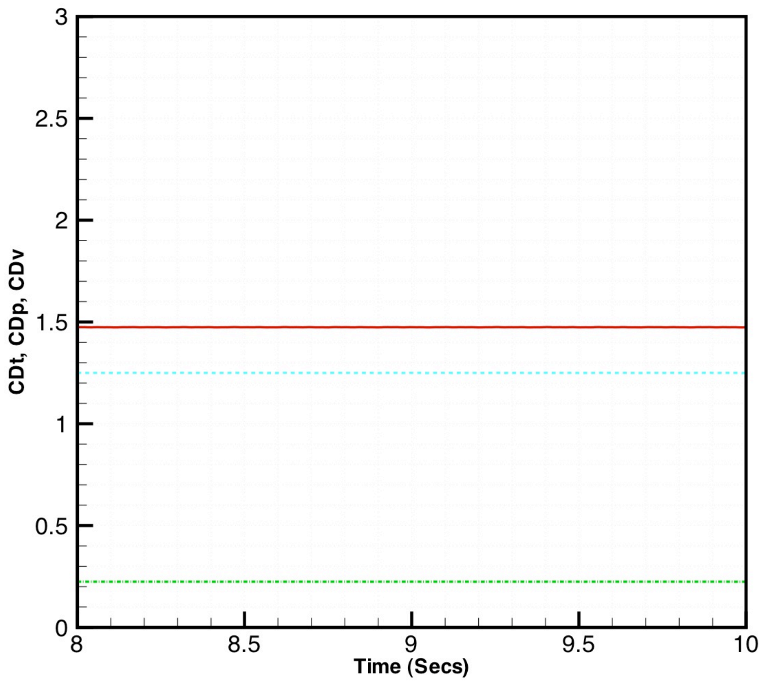

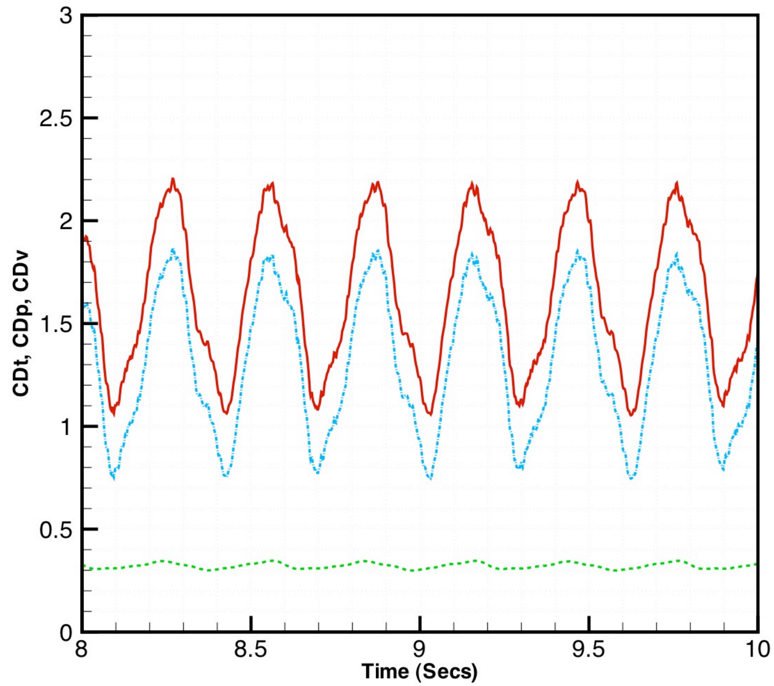

Comparison of drag time histories for rigid (left) and elastic (right) beam. Pressure component of CD curve is in dashed blue color line. The viscous component is in green dash-dot curve. Total CD is the red solid curve.

Applications

STANFORD UNIVERSITY

1. Parallelization using GPUs
2. Unsteady Flow on Deformable Meshes
3. Adaptive h-p Mesh Refinement
4. Implicit Large Eddy Simulation with SD
5. LES Models with SD

Adaptive hp Refinement Using Entropy Error Indicator (Fidkowski and Roe)

Cylinder, M = 0.3

Mortar Elements at Mismatched Interfaces

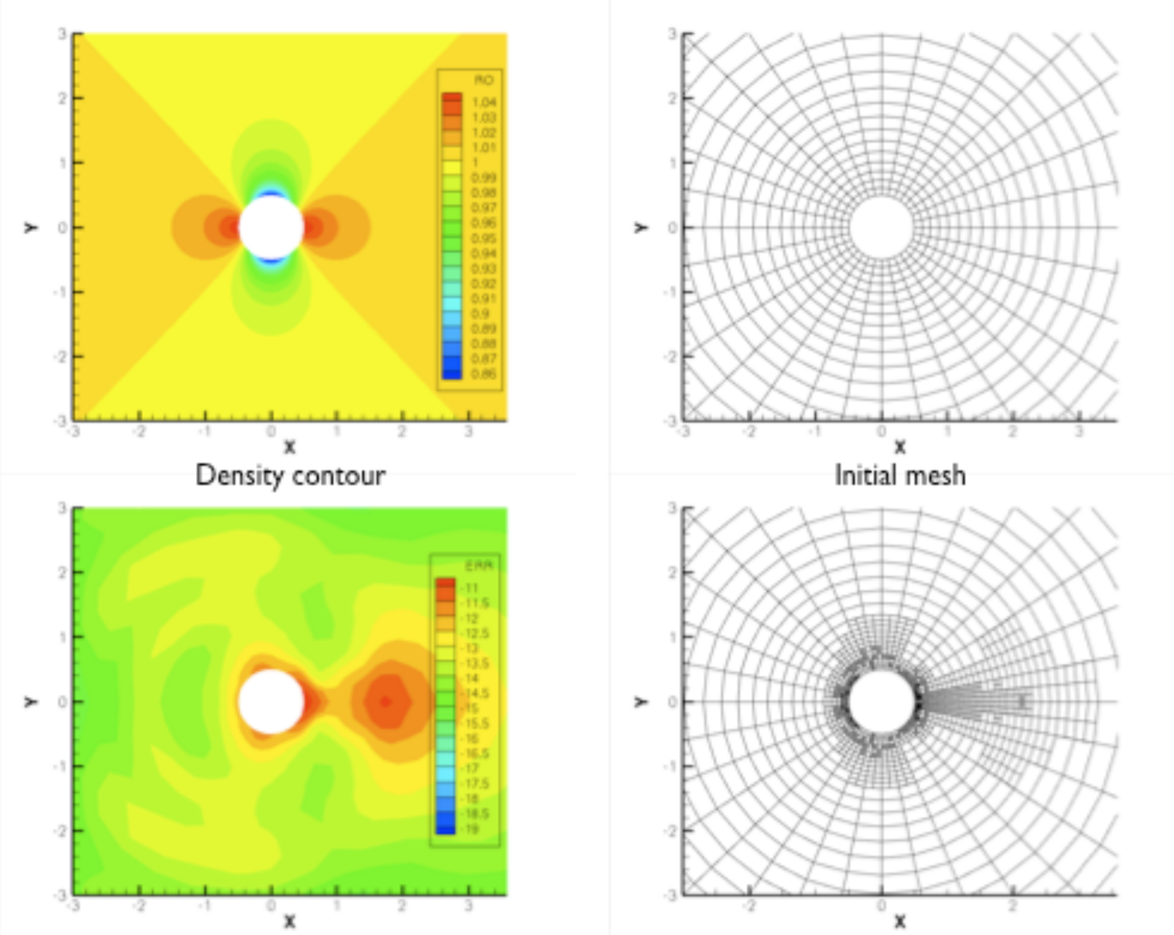

Density contour | Initial mesh | Initial error map | Mesh after 3 *h*-refinements

Adaptive p Refinement

STANFORD UNIVERSITY

Cylinder, M = 0.3

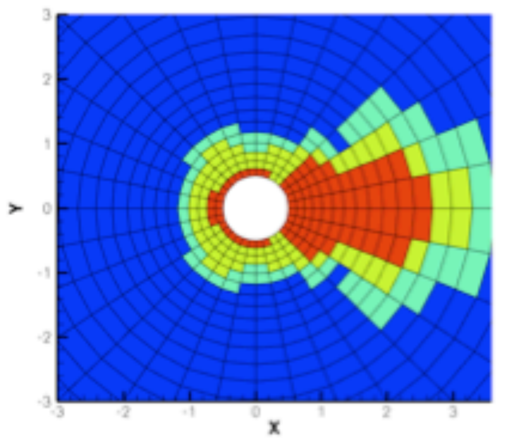

Order distribution after 3 *p*-refinements

With both refinement and coarsening, the order distribution becomes fragmented.

Too many interfaces with order mismatch result in reduced speed and accuracy.

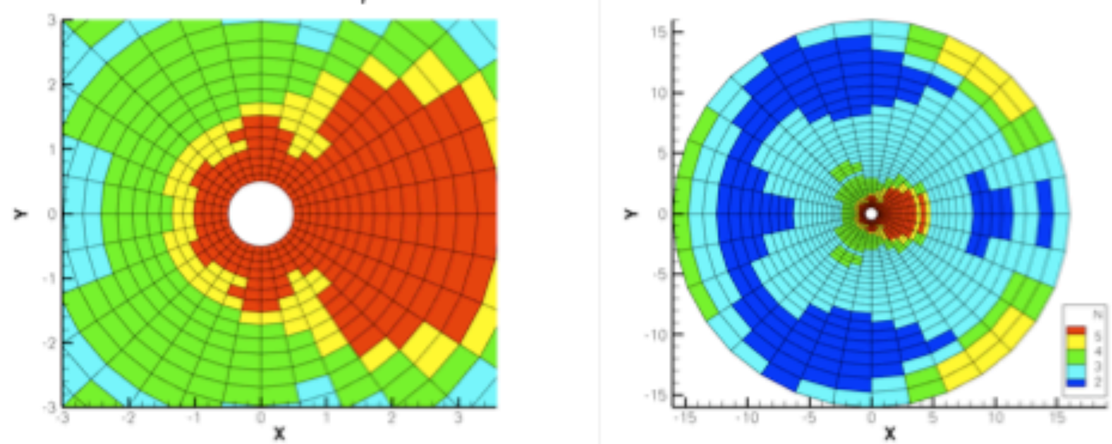

Order distribution after 3 *p*-adaptations, i.e. both refinements and coarsening

Adaptive p Refinement

STANFORD
UNIVERSITY

NACA 0012, M = 0.4, 5 deg

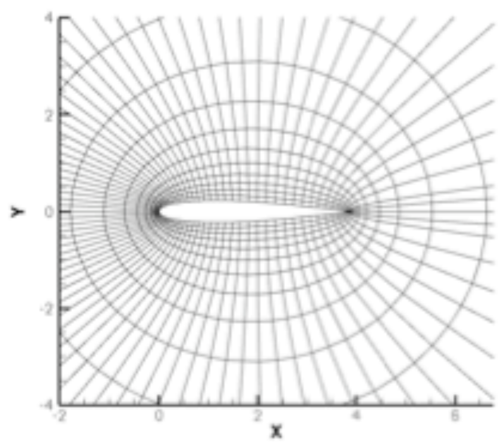

Initial mesh

Bottom left:

Initial error with N = 2

Bottom right:

Initial error with N = 3

(a more accurate initial solution)

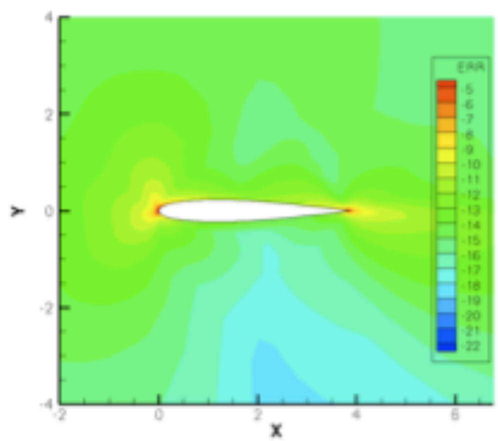

Initial error map with N = 2

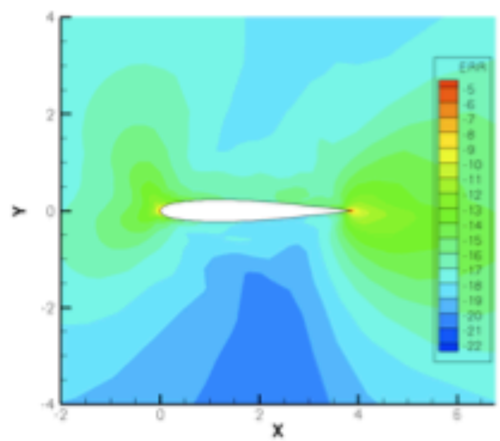

Initial error map with N = 3

Adaptive p Refinement

STANFORD
UNIVERSITY

NACA 0012, M = 0.4, 5 deg

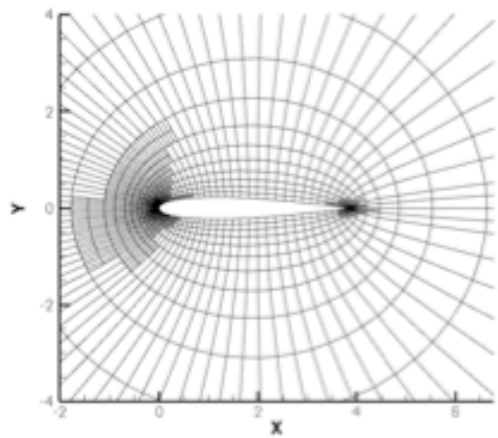

Mesh after 3 *h*-refinements, N = 2 initially

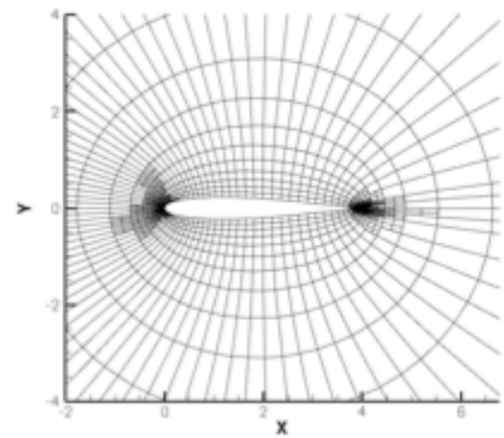

Mesh after 3 *h*-refinements, N = 3 initially

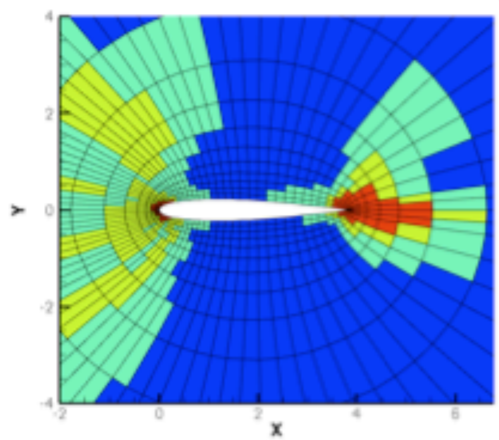

Order distribution after 3 *p*-refinements, N = 2 initially

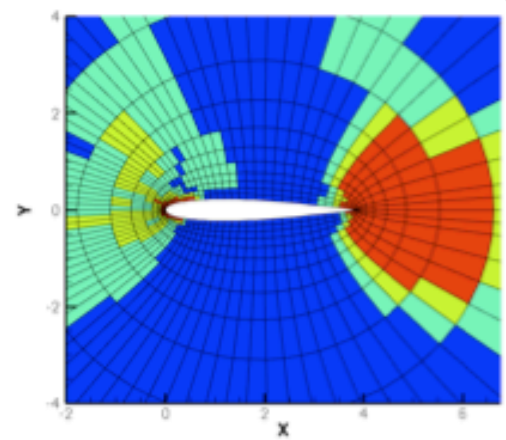

Order distribution after 3 *p*-refinements, N = 3 initially

Adaptive h Refinement

STANFORD UNIVERSITY

NACA 0012, M = 0.4, 5 deg

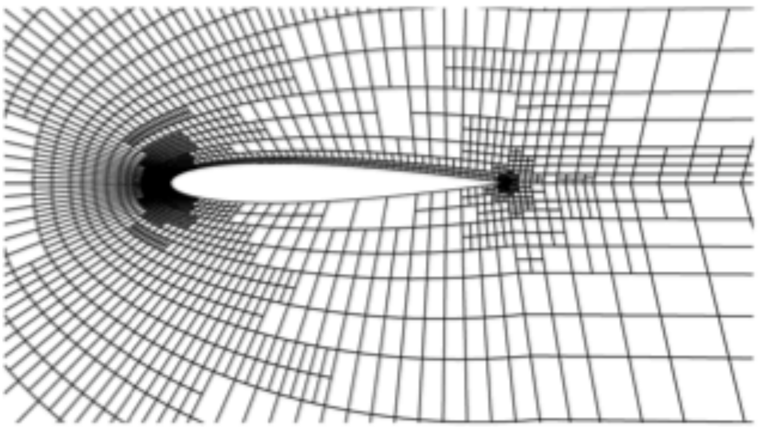

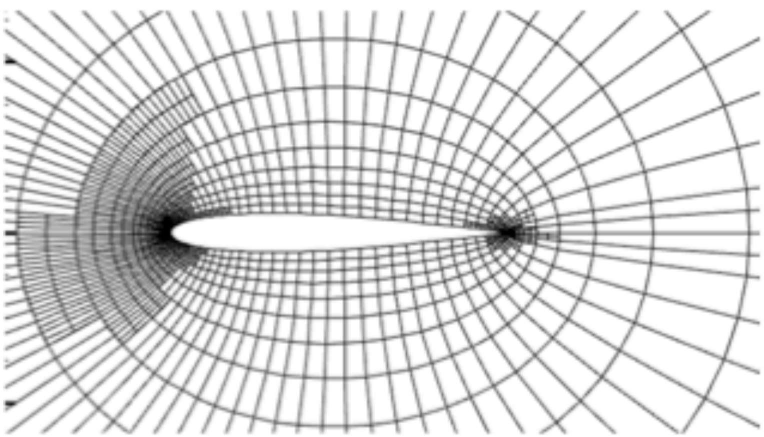

Comparison with Fidkowski and Roe's result

top: Fidkowski and Roe's

bottom: SD

- Initial N = 2
- 3 *h*-refinements

Adaptive h Refinement

Bump, M = 1.4

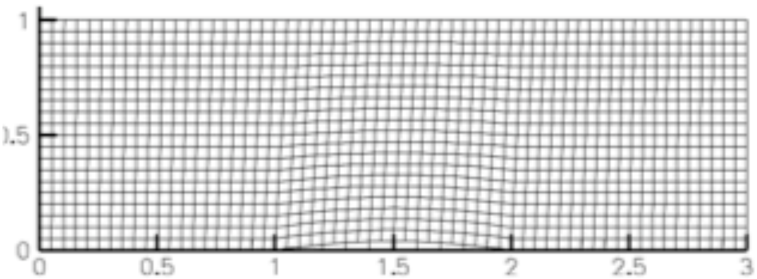

Initial mesh

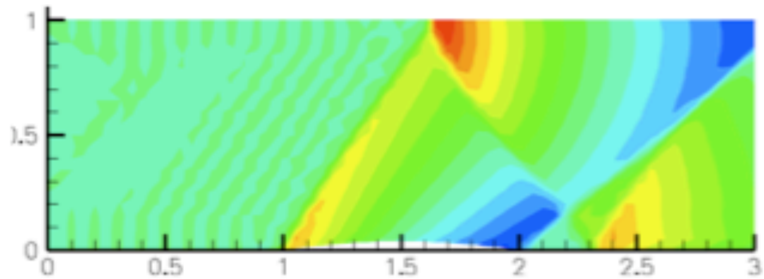

Density contour on the initial mesh

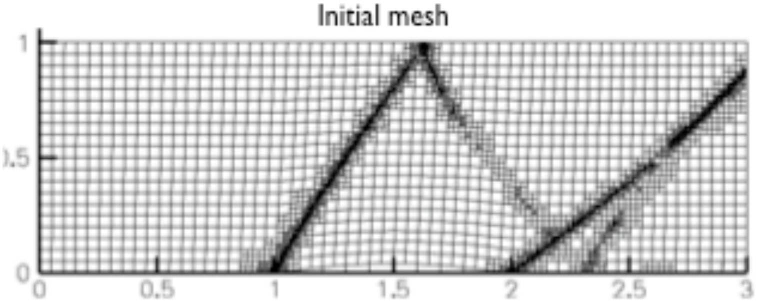

Mesh after 3 *h*-refinements

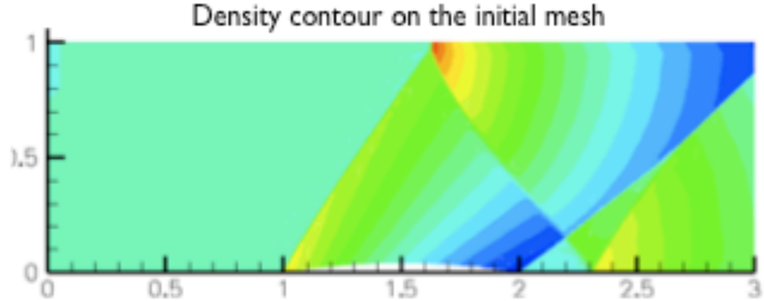

Density contour after 3 *h*-refinements

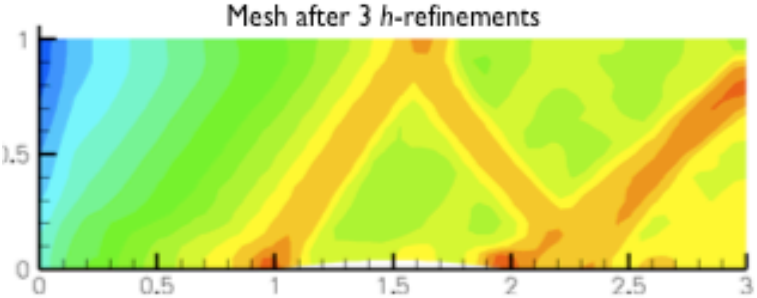

Initial error map

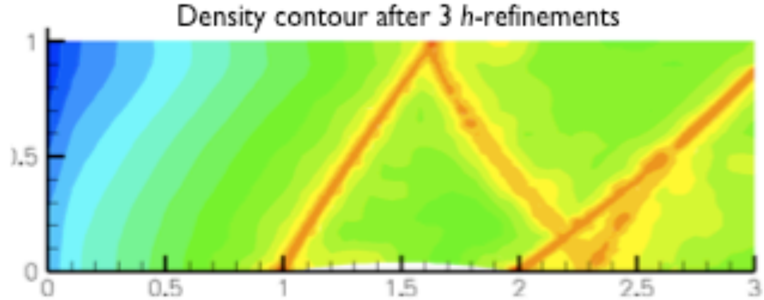

Error map after 2 h-refinements

Adaptive h Refinement

STANFORD
UNIVERSITY

NACA 0012, M = 0.8, 1.25 deg

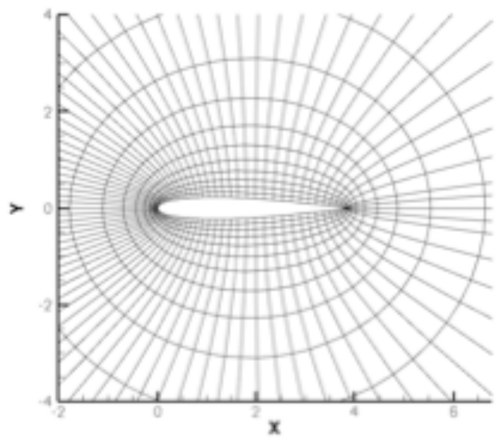

Initial mesh

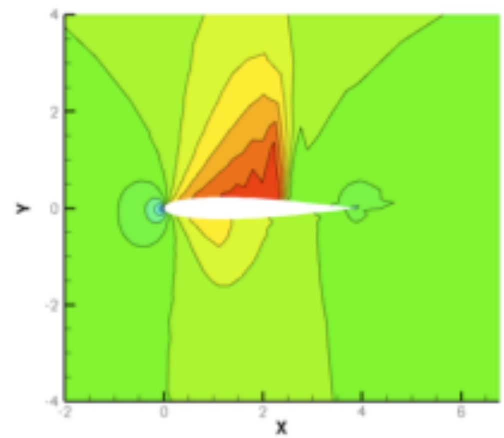

Mach contour on the initial mesh

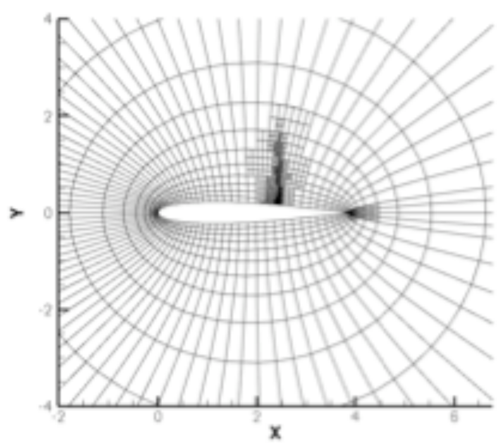

Mesh after 3 *h*-refinements

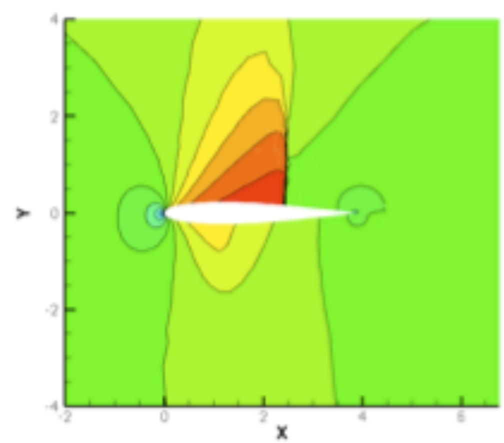

Mach contour after 3 *h*-refinements

Applications

STANFORD UNIVERSITY

1. Parallelization using GPUs
2. Unsteady Flow on Deformable Meshes
3. Adaptive h-p Mesh Refinement
4. Implicit Large Eddy Simulation with SD
5. LES Models with SD

Implicit Large Eddy Simulation with SD

STANFORD UNIVERSITY

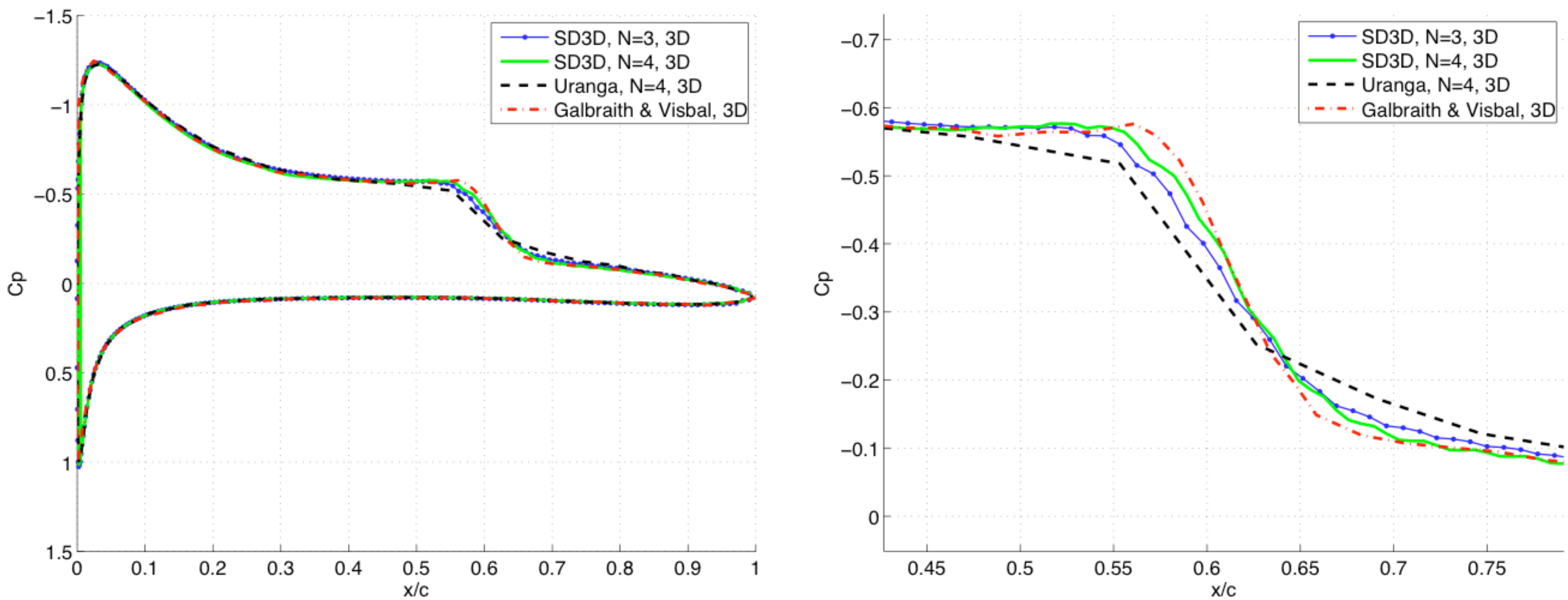

(a) (b) Zoomed In

Comparison of average pressure coefficient distribution at Re=60000, AOA=4

Implicit Large Eddy Simulation with SD

STANFORD UNIVERSITY

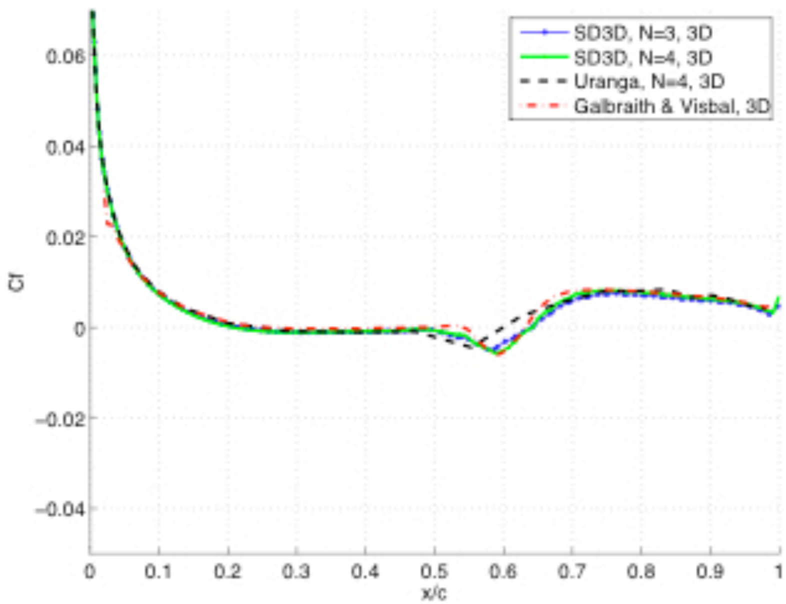

(a)

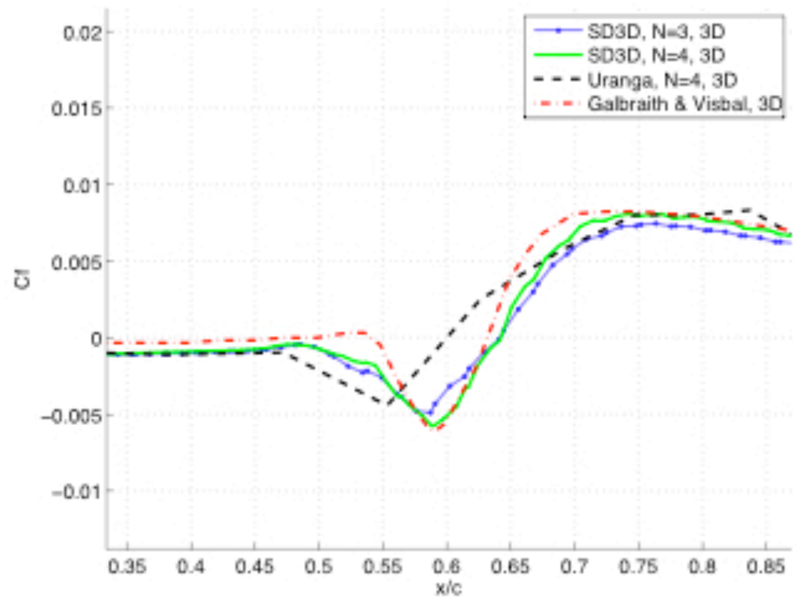

(b) Zoomed In

Comparison of average skin friction coefficient distribution at Re=60000, AOA=4

Implicit Large Eddy Simulation with SD

STANFORD UNIVERSITY

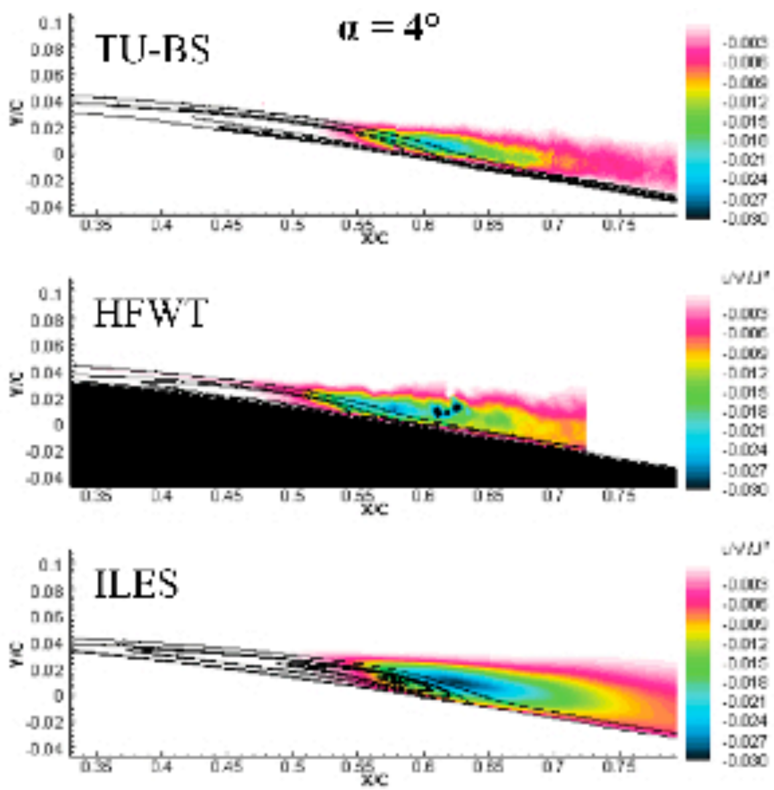

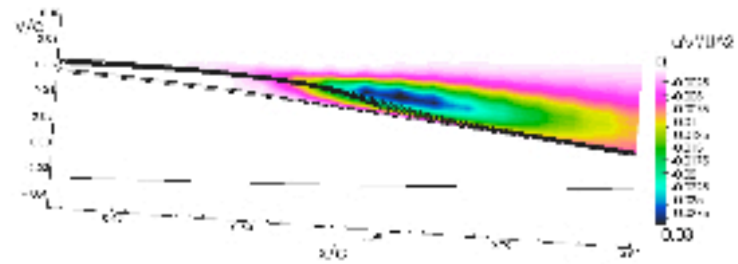

(a) N=3

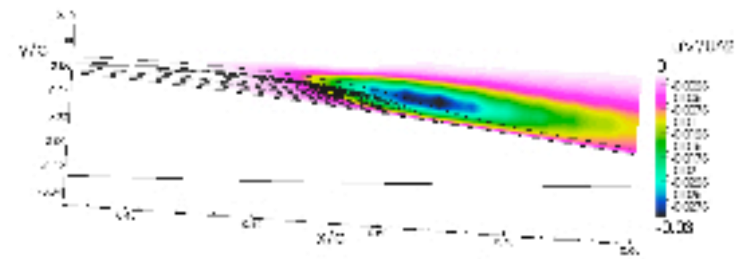

(b) N=4

Figure 11: Reynolds stress contours from HFWT and TU-BS experiments and computations by Galbraith and Visbal at $Re = 60000, \alpha = 4^{\circ}$

Figure 12: Reynolds stress contours using SD solver at $Re = 60000, \alpha = 4^{\circ}$

Good agreement of mean velocity profiles

Implicit Large Eddy Simulation with SD

STANFORD UNIVERSITY

Data Set	Freestream Turbulence	Separation x_{sep}	Transition x_{tr}/c	Reattachment x_r/c
TU-BS	0.08%	0.30	0.53	0.64
HFWT	0.1%	0.18	0.47	0.58
Yuan[1] SGS-LES	0	0.21	0.49	0.60
Yuan[1] RANS-e^N	0.1%,N=8	0.21	0.49	0.58
Lian[2] RANS-e^N	0.1%,N=8	0.21	0.48	-
Galbraith and Visbal, ILES	0	0.23	0.55	0.65
Uranga, ILES	0	0.23	0.51	0.60
Present ILES, N=3	0	0.23	0.52	0.65
Present ILES, N=4	0	0.23	0.52	0.65

Table 2: Measured and Computed properties of flow over SD7003 at Re=60000, $\alpha = 4^\circ$

[1] W. Yuan, M. Khalid, J. W. U. S. and Radespiel, R., *An Investigation of Low-Reynolds-number Flows past Airfoils*, Aiaa paper 2005-4607, 2005.

[2] Lian, Y. and Shyy, W., *Laminar-Turbulent Transition of a Low Reynolds Number Rigid or Flexible Airfoil*, AIAA paper 2006-3051, 2006.

Implicit Large Eddy Simulation with SD

STANFORD UNIVERSITY

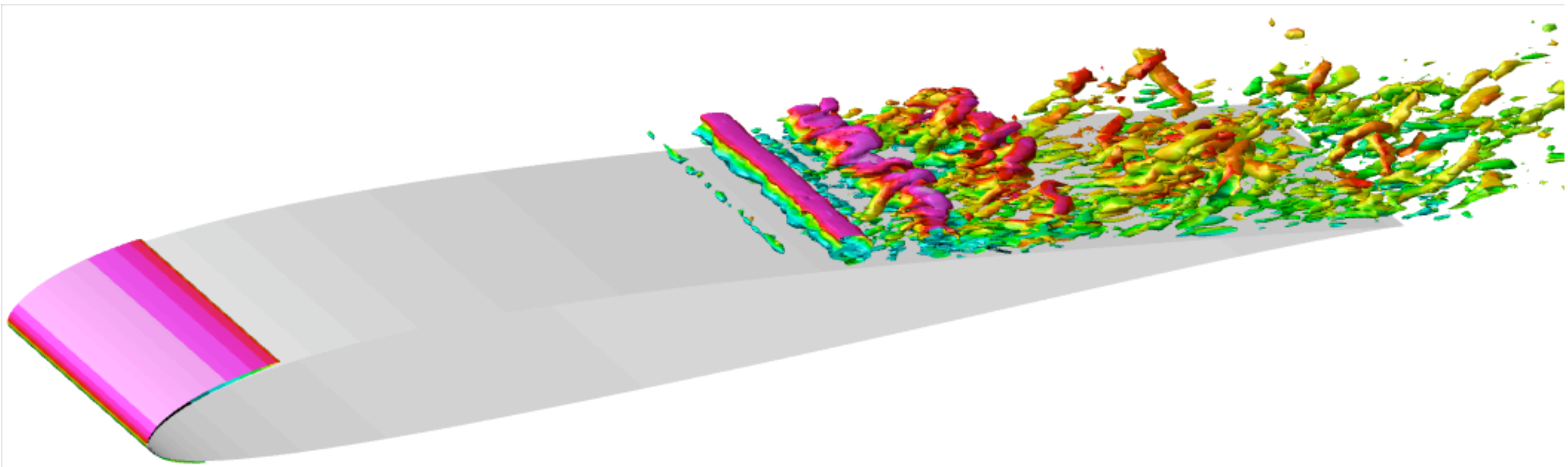

Instantaneous iso-surfaces of Q-criterion (Q=500) at Re = 60000, α = 4°

Applications

STANFORD UNIVERSITY

1. Parallelization using GPUs
2. Unsteady Flow on Deformable Meshes
3. Adaptive h-p Mesh Refinement
4. Implicit Large Eddy Simulation with SD
5. LES Models with SD

LES of flow over a cylinder at Re=2850 using SD Method with WALE and WSM Models

STANFORD UNIVERSITY

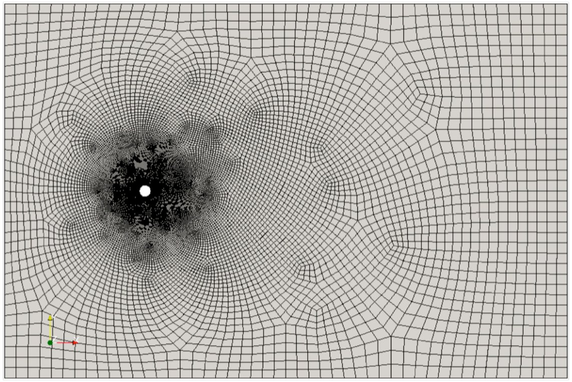

SD Methods with
WALE and
WALE Similarity Mixed (WSM) Models
Have Been Implemented

Figure 1: Computational domain: 24120 cells for a total of 651240 degrees of freedom. The grid extends from $-12D$ to $36D$ in the streamwise direction, from $-16D$ to $16D$ in the vertical direction and from $-1.6D$ to $1.6D$ in the spanwise direction, with the cylinder, of diameter D, centered at the origin.

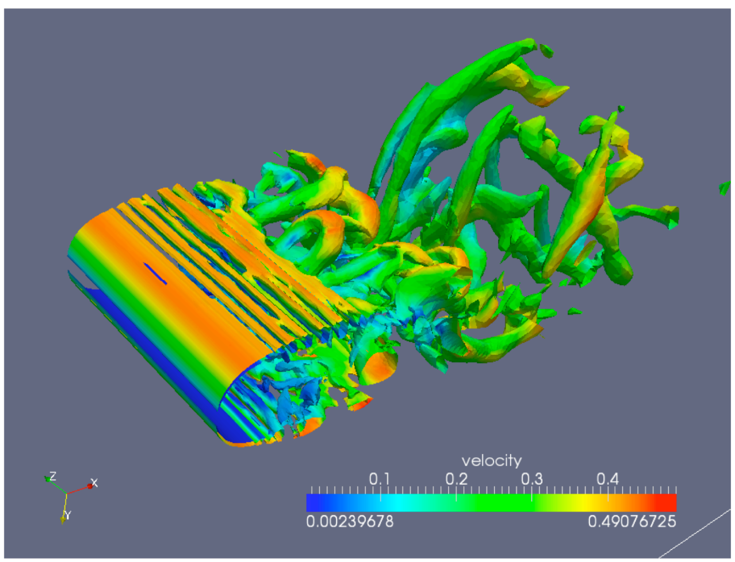

Figure 6: Instantaneous view of coherent vortical structures detaching from the cylinder colored by the local velocity magnitude.

LES of flow over a cylinder at Re=2850 with SD Method

STANFORD UNIVERSITY

Average Profile of Streamwise Velocity

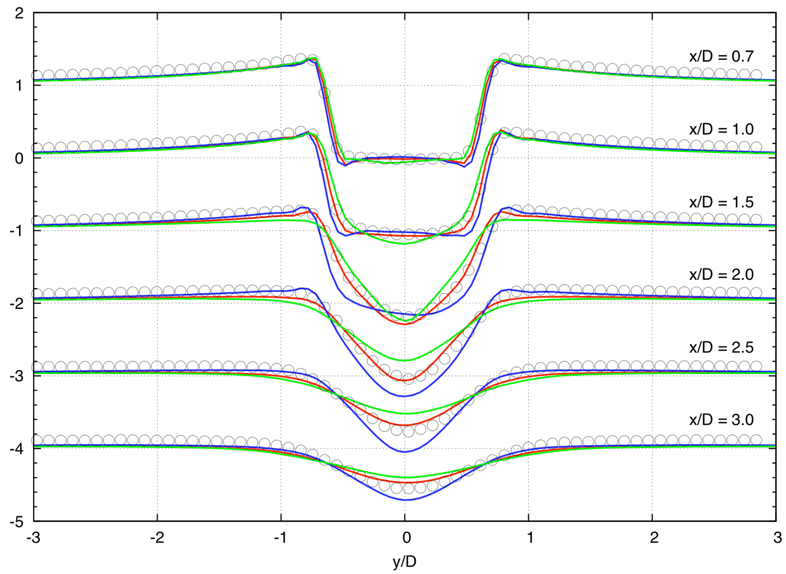

Figure 2: Average profiles of streamwise velocity, $\langle u\rangle/U_\infty$, measured at different locations downstream of the cylinder: red, WSM model; blue, WALE model; green, No model; $\circ$, experimental PIV measurements.

Streamwise Velocity Fluctuations

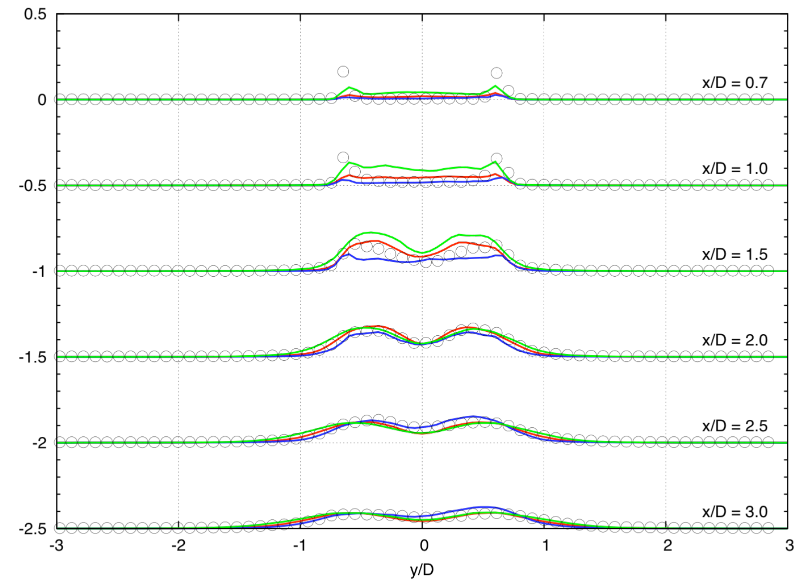

Figure 3: Profiles of streamwise velocity fluctuations, $\langle u'u'\rangle/U_\infty^2$, measured at different locations downstream of the cylinder: red, WSM model; blue, WALE model; green, No model; $\circ$, experimental PIV measurements.

Comparison of Experiment and SD Numerical Simulations without Model and with WSM and WALE Models

LES of flow over a cylinder at Re=2850 with SD Method

STANFORD UNIVERSITY

Profile of Velocity Cross correlation

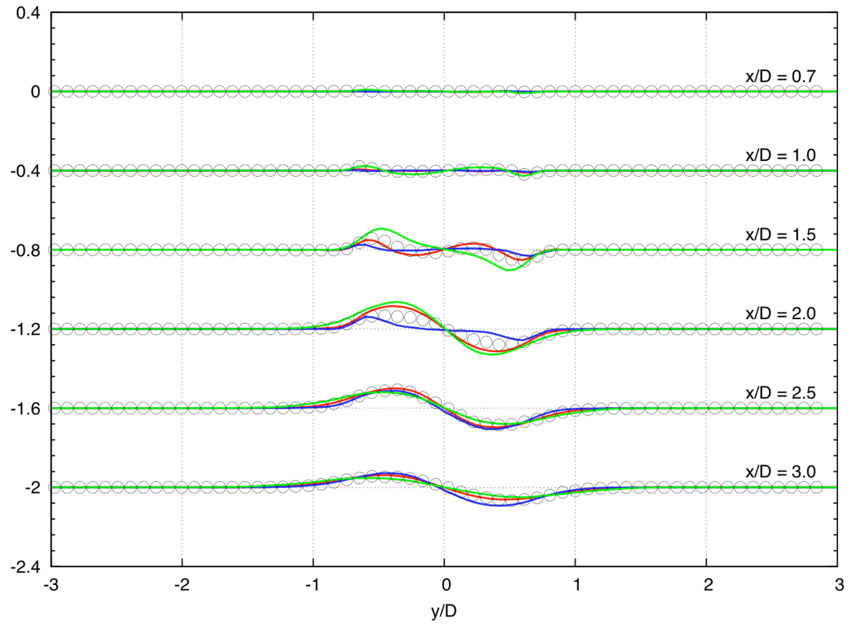

Figure 4: Profiles of velocity cross correlations, $\langle u'v' \rangle / U_\infty^2$, measured at different locations downstream of the cylinder: red, WSM model; blue, WALE model; green, No model; ○ , experimental PIV measurements.

Average Streamwise and Vertical Velocities

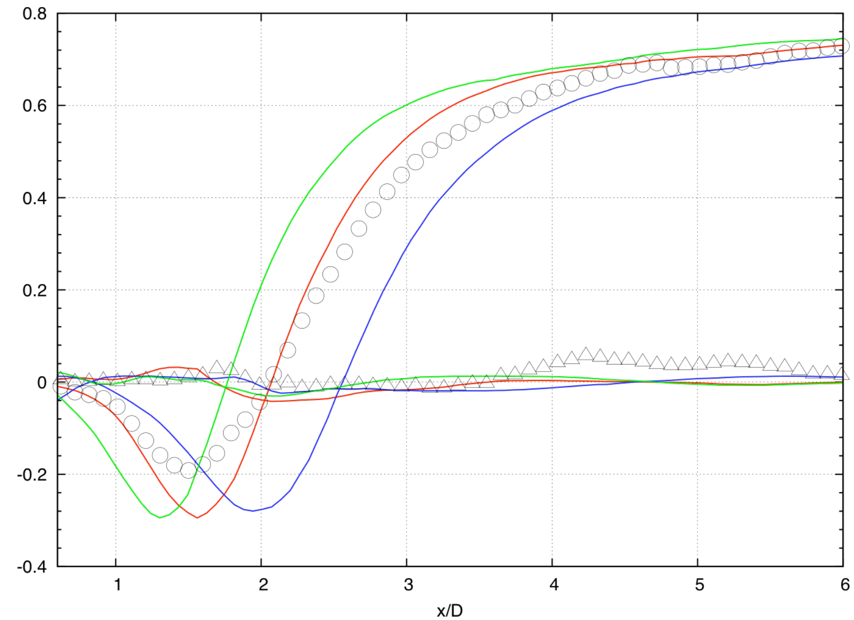

Figure 5: Average streamwise and vertical velocities measured along the wake of the cylinder at $y/D = 0$: red, WSM model; blue, WALE model; green, No model; ○ , △ , experimental PIV measurements.

Comparison of Experiment and SD Numerical Simulations without Model and with WSM and WALE Models

Conclusions

STANFORD UNIVERSITY

- On the theoretical side we have formulated a new approach to the construction of energy-stable high order schemes for arbitrary elements.
- On the practical side we have demonstrated significant improvements in the simulation of vortex dominated and transitional flows, including applications with deforming boundaries.
- Our goal is to develop a suite of software that will enable a new level of CFD in industrial practice.

Acknowledgments

STANFORD UNIVERSITY

- Air Force Office of Scientific Research
- National Science Foundation